Decay properties of hybrid mesons with a massive constituent gluon and search for their candidates

Shin Ishida and Haruhiko Sawazaki
Atomic Energy Research Institute, College of Science and Technology, Nihon University, Tokyo 101, Japan

Masuho Oda
Faculty of Engineering, Kokushikan University, Tokyo 154, Japan

Kenji Yamada
Department of Computer and Information Science, Junior College Narashino Campus, Nihon University, Funabashi, Chiba 274, Japan

(Received 27 December 1991)

In a previous work we argued the possibility of the $f_1(1420)$ being our first hybrid meson with the configuration of $(u\bar{u}+d\bar{d})g/\sqrt{2}$, and gave a preliminary consideration to search for other hybrid mesons. In this paper we calculate respective decay widths of the other members of ground-state hybrid-meson nonets in the framework of the covariant oscillator quark model extended to describe bound systems composed of quarks, antiquarks, and/or gluons. Based upon these results we select eight "observed" candidates altogether, three of them on a rather firm basis, and give some remarks to search further for their candidates experimentally.

PACS number(s): 14.40.−n, 12.40.Aa, 12.40.Qq, 13.25.+m

I. INTRODUCTION

Recently, there has been an overwhelming belief among particle physicists that the strong interaction among hadrons is fundamentally described by quantum chromodynamics (QCD). However, we feel that QCD in its present stage still needs more evidence and further development to be accepted as the fundamental final theory. It is one of the most serious theoretical problems that the present theory of QCD does not actually solve the confinement problem, since there have been no established methods for rigorous treatment of relativistic bound states, though all experimental observations are made only through hadrons as composite states of constituent quarks and/or antiquarks.

In this paper we shall concern ourselves with another more phenomenological but important problem. A characteristic feature of QCD, compared to quantum electrodynamics (QED), is that gluons, mediators of the color force, themselves have color charge as well as quarks and antiquarks, while in QED photons have no electric charge. So it is quite plausible that there exist gluonic hadrons [1], namely, glueballs and hybrids, which contain gluons as their constituents, in addition to ordinary hadrons with only quarks and/or antiquarks. If their existence is confirmed experimentally, it will add strong evidence for QCD to be the true theory.

A useful clue for searching gluonic states is obtained by careful examination of the ordinary hadron spectrum. Concerning the level spectrum of ordinary $q\bar{q}$ mesons, only the ground S-wave states, whose masses are lower than 1 GeV, have been confirmed completely, while the excited states, even the next P-wave ones, have been confirmed only partially. Recently, as experiments have gotten more accurate, there have been observed [2] too many mesons to be assigned as $q\bar{q}$ mesons in the mass region of 1–2 GeV. In Table I we show the present status of assignments to the P-wave $q\bar{q}$-meson nonets, while in Table II are collected still-unclassified mesons with positive parity and a mass of about 1.0–1.6 GeV. By comparison between these two tables, we see that, for the isoscalar partner (with mainly $s\bar{s}$ content) of the $f_1(1285)$ in the $^3P_1$ $q\bar{q}$ nonet, there exist two candidates, which are well confirmed experimentally.

In our previous paper [3], we have given the argument that the $f_1(1420)$ out of the above two is classified as our "first" hybrid meson with the configuration of $(u\bar{u}+d\bar{d})g/\sqrt{2}$ [u ($\bar{u}$), d ($\bar{d}$), and g being u ($\bar{u}$) quark, d ($\bar{d}$) quark, and gluon, respectively], while the remaining $f_1(1510)$ is classified as a member of the $^3P_1$ $q\bar{q}$ nonet.

TABLE I. Present status of assignments for the P-wave $q\bar{q}$-meson nonets.

		$I=1$	$I=\frac{1}{2}$	$I=0$	
$^{2S+1}L_J$	J^{PC}	$n\bar{n}$	$n\bar{s},s\bar{n}$	$n\bar{n}$	$s\bar{s}$
$^1P_1$	1^{+-}	$b_1(1235)$	$K_1(1400)$	$h_1(1170)$	$h_1(1380)$
$^3P_0$	0^{++}		$K_0^*(1430)$?	$f_0(1400)$?	
$^3P_1$	1^{++}	$a_1(1260)$	$K_1(1270)$	$f_1(1285)$	
$^3P_2$	2^{++}	$a_2(1320)$	$K_2^*(1430)$	$f_2(1270)$	$f_2'(1525)$

TABLE II. Unclassified observed mesons with positive parity and a mass of about 1.0–1.6 GeV. The data are taken from Ref. [28], unless otherwise noted.

J^{PC}	Meson	Mass (MeV)	Total width (MeV)	Main observed modes
1^{+-}	$b_1(1310)$[a]	1311±10	126±10	$\eta(\pi\pi)_P$
	$K_1(1650)$[b]	1650±50	150±50	ϕK
0^{++}	$a_0(980)$	983±3	57±11	$\eta\pi, K\bar{K}$
	$a_0(1320)$	1322±30	130±29	$\eta\pi$
	$f_0(975)$	976±3	34±6	$\pi\pi, K\bar{K}$
	$f_0(1240)$	1240±22	140±22	$K\bar{K}$
	$f_0(1525)$	≈1525	≈90	$K\bar{K}$
	$f_0(1590)$	1587±11	175±19	$\eta\eta', \eta\eta, 4\pi^0$
1^{++}	$f_1(1420)$	1422±10	55±3	$K^*\bar{K}$
	$f_1(1510)$	1512±4	35±15	$K^*\bar{K}$
2^{++}	$f_2(1430)$	≈1430	≈10–150	$\pi\pi, K\bar{K}$
	$f_2(1565)$	1565±10	170±20	$\pi\pi$
	$f_2(1640)$	1635±7	<70	$\omega\omega$

[a]Reference [26].
[b]Although this meson is not an eigenstate of charge conjugation, it is put here for the sake of convenience.

There we have also given some theoretical arguments to search for other hybrid mesons, based upon preliminary calculations of their decay widths in the covariant oscillator quark model [4] (COQM) extended [3] so as to be applicable to systems containing massive vector constituents. In this paper we shall give the results of more complete calculations of their decay widths and try to give more rigorous general arguments to search for hybrid mesons, which may give a new powerful viewpoint in investigating meson spectroscopy.

The contents of this paper are as follows. In Sec. II we present the formulation of the extended COQM and describe the level structure of hybrid mesons. It is also pointed out that there occurs an interesting phenomenon of "doubling of four flavor nonets" between the P-wave $q\bar{q}$ states and the ground hybrid $q\bar{q}g$ ones. In Sec. III covariant effective Hamiltonians are systematically derived for respective processes of the ground-state hybrid mesons decaying into two S-wave $q\bar{q}$ mesons in the extended COQM. Then the respective partial decay widths and total widths as their sums are calculated by using the observed decay width of the $f_1(1420)$ as input. In Sec. IV, based upon these predicted decay properties of hybrid mesons, we select several other candidates out of the observed meson resonances. Then, as a clue to search further for their candidates experimentally, several remarks based upon the above results are given. Finally, in Sec. V some concluding remarks are given.

II. MODEL SCHEME FOR HYBRID MESONS AND THEIR SPECTRUM

A. Extended covariant oscillator quark model

We regard [3,5] hybrid $q\bar{q}g$ mesons [6] as color-singlet three-body bound states, confined by a harmonic potential, of a quark, an antiquark, and a gluon with respective "constituent" masses and treat them in the framework of the extended COQM. Needless to say, in order to treat nonstatic problems such as decay processes, it is indispensable to describe them in a covariant framework. The COQM has [4] a long history of development and has been applied to various problems with satisfactory results. The basic standpoints of our extended COQM are as follows: (1) The constituent quarks and gluons have their respective effective masses dynamically generated inside hadrons; (2) the level structures of composite systems are well described by the spin-orbit (L-S) coupling scheme; (3) the confinement potential is of a four-dimensional harmonic-oscillator type.

The idea that the gluon has an effective mass has been advocated [7] in continuum QCD, and it has been actually shown [8] in the numerical studies of the gluon propagator in lattice QCD. This idea has also been supported [9] by a phenomenological point of view. The effective mass value is in the range of about 500–800 MeV according to these analyses. Nonrelativistic quark models (NRQM's) with the L-S coupling scheme have been successful in explaining static properties of hadrons. In order to sustain these successes, the framework is extended to the boosted L-S coupling scheme in the extended COQM, where the spin (now including the spin of gluons in addition to of quarks) and space-time parts of the wave functions are covariantly extended, separately, from the corresponding parts of the NRQM.

The hybrid mesons are systematically described by a trilocal field (wave function) as

$$H^{\beta}_{\alpha,\nu}(x_1,x_2,x_3)\ , \tag{2.1}$$

where x_1, x_2, and x_3 are the Lorentz four-vectors representing the space-time coordinates of a constituent

quark, antiquark, and gluon, respectively. This wave function satisfies [10] the Bargmann-Wigner equations concerning the quark and antiquark spin indices α and β ($\alpha,\beta=1-4$) as

$$(iP_\mu\gamma_\mu^{(1)}+M)_\beta^{\alpha'}H_{\alpha',\nu}^{\beta}=0 ,$$
$$\bar{H}_{\alpha',\nu}^{\beta}(iP_\mu\gamma_\mu^{(2)}-M)_\beta^{\alpha'}=0 , \tag{2.2}$$

where $\gamma_\mu^{(1)}$ and $\gamma_\mu^{(2)}$ ($\mu=1-4$) are the Dirac matrices (we use the Dirac-Pauli Hermitian representation, that is, $\gamma_\mu^\dagger=\gamma_\mu$) and $\bar{H}\equiv H^*\gamma_4^{(1)}\gamma_4^{(2)}$. For simplicity, the color and flavor indices are omitted through this paper. It also satisfies the Lorentz condition concerning the gluon spin index ν ($\nu=1-4$) as

$$P_\nu H_{\alpha,\nu}^{\beta}=0 . \tag{2.3}$$

It is noted that in Eqs. (2.2) and (2.3) P_μ represents the center-of-mass momentum of hybrid mesons and in Eq. (2.2) M is the mass of relevant hybrid mesons, which is determined through the following space-time wave equation [11] to be satisfied by the wave function of Eq. (2.1):

$$\left[\sum_{i=1}^{3}\frac{1}{2m_i}\frac{\partial^2}{\partial x_{i\mu}^2}-U(x_1,x_2,x_3)\right]H_{\alpha,\nu}^{\beta}(x_1,x_2,x_3)=0 , \tag{2.4}$$

where m_i is the mass parameter for the ith constituent. Here U is the potential working among the constituents and is supposed to be

$$U=U_{\rm conf}+U_{\rm PQCD} ,$$
$$U_{\rm conf}=-\tfrac{3}{4}\sum_{i>j}\tfrac{1}{2}K(x_i-x_j)_\mu^2\mathbf{T}_i\cdot\mathbf{T}_j+C , \tag{2.5}$$

where $U_{\rm conf}$ ($U_{\rm PQCD}$) stands for the confinement (perturbative QCD) potential, K represents the parameter for the confining strength, C is the constant parameter, and $\mathbf{T}_i$ ($\mathbf{T}_i\rightarrow-\mathbf{T}_i^*$ for antiquarks) are the color-SU(3) generators. In this work, $U_{\rm PQCD}$ will be neglected.

Defining the center-of-mass coordinate $X_{H\mu}$ and relative coordinates ρ_μ and λ_μ as

$$X_{H\mu}=\frac{1}{m_1+m_2+m_3}(m_1x_1+m_2x_2+m_3x_3)_\mu , \tag{2.6a}$$

$$\rho_\mu=\frac{1}{\sqrt{2}}(x_1-x_2)_\mu , \tag{2.6b}$$

$$\lambda_\mu=\left[\frac{2}{3}\right]^{1/2}\left[\frac{1}{m_1+m_2}(m_1x_1+m_2x_2)-x_3\right]_\mu , \tag{2.6c}$$

the wave equation (2.4) is rewritten in the Klein-Gordon form

$$\left[\frac{\partial^2}{\partial X_{H\mu}^2}-\mathcal{M}^2(\rho_\mu,\lambda_\mu)\right]H_{\alpha,\nu}^{\beta}(X_{H\mu},\rho_\mu,\lambda_\mu)=0 , \tag{2.7a}$$

with the mass-squared operator

$$\mathcal{M}^2(\rho_\mu,\lambda_\mu)=dH_0 , \tag{2.7b}$$

where

$$d=2\sum_{i=1}^{3}m_i \tag{2.8a}$$

and

$$H_0=-\frac{1}{2m}\frac{\partial^2}{\partial\rho_\mu^2}-\frac{1}{2m_\lambda}\frac{\partial^2}{\partial\lambda_\mu^2}+\frac{3}{2}K_\rho\rho_\mu^2+\frac{3}{2}K_\lambda\lambda_\mu^2+C , \tag{2.8b}$$

with

$$K_\rho=\tfrac{7}{24}K , \quad K_\lambda=\tfrac{9}{8}K , \quad m_\lambda=\frac{3mm_g}{2m+m_g} . \tag{2.8c}$$

In Eqs. (2.8b) and (2.8c), we have given an expression for the simple case of $m_1=m_2\equiv m$ ($m_3\equiv m_g$). As mentioned above, in Eq. (2.7) the eigenvalues of $\mathcal{M}^2$ give the masses squared of hybrid mesons. In order to freeze the redundant freedom of relative time, we require the definite-metric-type subsidiary condition [12] for the wave function

$$P_\mu a_\mu^{(\rho,\lambda)\dagger}|H\rangle=0 , \tag{2.9}$$

where P_μ is the center-of-mass momenta of hybrid mesons and $a_\mu^{(\rho,\lambda)\dagger}$ are the creation operators for relative harmonic motions concerning the ρ and λ coordinates. As is well known, the wave function satisfying this condition is normalizable and gives [13] the electromagnetic form factors of hadrons with the desirable asymptotic behavior.

B. Level structures of hybrid mesons and doubling of states between the *P*-wave $q\bar{q}$ mesons and ground-state hybrid $q\bar{q}g$ mesons

The level structures of hybrid mesons are described by the wave equations of Eqs. (2.2), (2.3), and (2.7). The essential structure is given by two four-dimensional harmonic oscillators concerning the relative coordinates ρ and λ. The total spin J of hybrid mesons is given as a sum of the two orbital angular momenta L_ρ and L_λ, the spin of the quark-antiquark subsystem S ($=0$ or 1), and the spin of the gluon S_g ($=1$). The parity is given by

$$P=(-1)^{L_\rho+L_\lambda} , \tag{2.10}$$

while the charge-conjugation parity of the neutral states is given by

$$C=(-1)^{L_\rho+S+1} . \tag{2.11}$$

In Table III we have shown the level structure up to the first excited states. Here it is worthwhile to note that in the first excited level there exist exotic J^{PC} states which never appear in $q\bar{q}$ states.

The mass of the ground states may be estimated simply as a sum of the masses of their constituents:

$$M_0(q\bar{q}g)=m_q+m_{\bar{q}}+m_g , \tag{2.12}$$

taking the values $m_n=385$ MeV (half of the ρ-meson mass) for n quarks (n denoting u or d quark), $m_s=510$ MeV (half of the ϕ-meson mass) for s quarks, and

TABLE III. Level structures of hybrid mesons. Exotic quantum number states are underlined. The mass range for respective levels is estimated in a way described in the text.

N[a]	L_ρ	L_λ	S	Σ[b]	J^{PC}			Mass (GeV)
			0	1	1^{+-}			
0	0	0		0	0^{++}			1.3–1.8
			1	1	1^{++}			
				2	2^{++}			
			0	1	0^{-+}	$\underline{1^{-+}}$	2^{-+}	
	1	0		0		1^{--}		1.8–2.2
			1	1	$\underline{0^{--}}$	1^{--}	2^{--}	
				2	1^{--}	2^{--}	3^{--}	
1								
			0	1	$\underline{0^{--}}$	1^{--}	2^{--}	
	0	1		0		$\underline{1^{-+}}$		2.0–2.4
			1	1	0^{-+}	$\underline{1^{-+}}$	2^{-+}	
				2	$\underline{1^{-+}}$	2^{-+}	$\underline{3^{-+}}$	

[a] $N=N_\rho+N_\lambda$.
[b] $\Sigma=S+S_g$.

$m_g=500-800$ MeV for gluons. Here it may be notable that the mass of the $f_1(1420)$ is just within the range of 1270–1570 MeV estimated this way.

The mass of the first excited states may be estimated, using the mass formula derived from Eqs. (2.7) and (2.8), by

$$M^2(q\bar{q}g)=M_0^2(q\bar{q}g)+N_\rho\Omega_{q\bar{q}g}^{(\rho)}+N_\lambda\Omega_{q\bar{q}g}^{(\lambda)}\ , \tag{2.13a}$$

with

$$\Omega_{q\bar{q}g}^{(\rho)}=\frac{\sqrt{7}}{8}\left[2+\frac{m_g}{m}\right]\Omega_{q\bar{q}}\ ,$$
$$\Omega_{q\bar{q}g}^{(\lambda)}=\frac{3}{8}\left[2+\frac{m_g}{m}\right]\left[\frac{2m+m_g}{m_g}\right]^{1/2}\Omega_{q\bar{q}}\ , \tag{2.13b}$$

where N_ρ (N_λ) and $\Omega^{(\rho)}$ ($\Omega^{(\lambda)}$) are, respectively, the number and the value of ρ (λ) oscillator quantum and $\Omega_{q\bar{q}}=\sqrt{32mK}$. Here the values of $\Omega^{(\rho)}$ and $\Omega^{(\lambda)}$ are

$$\Omega_{n\bar{n}g}^{(\rho)}\approx 1.26\Omega_{n\bar{n}}\approx 1.45\ \text{GeV}^2\ ,$$
$$\Omega_{n\bar{n}g}^{(\lambda)}\approx 2.07\Omega_{n\bar{n}}\approx 2.39\ \text{GeV}^2\ \text{for}\ n\bar{n}g\ \text{systems}\ , \tag{2.14a}$$

$$\Omega_{s\bar{s}g}^{(\rho)}\approx 1.12\Omega_{s\bar{s}}\approx 1.48\ \text{GeV}^2\ ,$$
$$\Omega_{s\bar{s}g}^{(\lambda)}\approx 1.98\Omega_{s\bar{s}}\approx 2.62\ \text{GeV}^2\ \text{for}\ s\bar{s}g\ \text{systems}\ , \tag{2.14b}$$

which are obtained by using the value of $\Omega_{n\bar{n}}=1.15\ \text{GeV}^2$ determined from the ρ-meson trajectory and the tentatively fixed value of $m_g=700$ MeV and by simply assuming the potential strength K to be flavor independent. In Table III we have shown the mass range of respective levels estimated as above (without discriminating quark flavor).

Finally, in this subsection we point out an interesting and important feature of the level structure in our scheme. The ground states of our hybrid mesons have completely the same quantum numbers as the P-wave $q\bar{q}$ mesons. This is due to the fact that a massive S-wave gluon inside the hybrid mesons plays a similar role to a P-wave quantum in the $q\bar{q}$ mesons. Moreover, the mass of the ground-state hybrid mesons is expected to be in the range of 1.3–1.8 GeV, which is just the mass range for the P-wave $q\bar{q}$ mesons. Thus, in such a mass region, there exists the doubling of four flavor nonets with quantum numbers $J^{PC}=(0,1,2)^{++}$ and 1^{+-} between the hybrid and the $q\bar{q}$ mesons with nearly equal masses with each other.

It is notable that in our model the lowest-lying states have positive parity. This is in strong contrast to the bag model, where the corresponding states have negative parity and are expected to lie in the mass range of 1–2 GeV [14]. In the case of the MIT bag model, there are two modes of gluon: namely, transverse electric (TE) mode and transverse magnetic (TM) one. TE and TM modes are due to the multipole expansion of the color-electromagnetic field inside the bag. The parity of the TE dipole mode, which is expected to be of the lowest energy, is given by $P_{\text{TE}}=(-1)^{J+1}=+$; accordingly, the ground-state hybrid mesons have negative parity. Actually, in an attempt based on the MIT bag model, the $f_1(1420)$, supposing it to have negative parity, was assigned to its ground state [15].

III. DECAY PROPERTIES OF THE GROUND-STATE HYBRID MESONS

A. Decay mechanism

Now we investigate the decays of hybrid $q\bar{q}g$ mesons into the two ordinary $q\bar{q}$ mesons, $H\rightarrow M_B+M_C$, in our model scheme. We assume [3,16] that these decays proceed by the conversion of the gluon into a $q\bar{q}$ pair as shown in Fig. 1. Then the invariant effective action for all the relevant interactions is given, in a unified manner, by the overlap integral

$$I_{\rm int}=\int d^4x_1d^4x_2d^4x_3[\overline{\Phi_\beta^{(C)\delta}}(x_3,x_2)(\Gamma_{3\nu})_\delta^\gamma\overline{\Phi_\gamma^{(B)\alpha}}(x_1,x_3)H_{\alpha,\nu}^\beta(x_1,x_2,x_3)+\text{H.c.}]\ , \tag{3.1}$$

where $\Phi_\gamma^{(B)\alpha}(x_1,x_3)$, etc., are the bilocal fields (wave functions) describing all the states in the final $q\bar{q}$ mesons and Γ_ν is the quark-gluon vertex operator [17] given as a sum of two terms corresponding to the "color-electric" and "color-magnetic" currents:

$$\Gamma_{i\mu}=\Gamma_{i\mu}^E+\Gamma_{i\mu}^M\ , \tag{3.2}$$

with

$$\Gamma_{i\mu}^E=-ig\left[\frac{\lambda_i^a}{2}\right]\frac{1}{2m_i}\left[\frac{\vec{\partial}}{\partial x_{i\mu}}-\frac{\overleftarrow{\partial}}{\partial x_{i\mu}}\right]\ , \tag{3.3a}$$

$$\Gamma_{i\mu}^M=-ig\left[\frac{\lambda_i^a}{2}\right]\frac{1}{2m_i}h_M(i\sigma_{\mu\nu}^{(i)})\left[\frac{\vec{\partial}}{\partial x_{i\nu}}+\frac{\overleftarrow{\partial}}{\partial x_{i\nu}}\right]\ , \tag{3.3b}$$

where g is the effective quark-gluon coupling constant, h_M is the dimensionless parameter corresponding to the effective quark color-magnetic moment (in the case of the normal moment, $h_M=1$), and λ_i^a is the color-SU(3) matrix.

Thus we can express the decay widths for all relevant possible channels in terms of the two coupling parameters g and h_M. Actually, we estimate only the decay widths of the ground-state hybrid mesons into the two S-wave $q\bar{q}$ mesons. We would expect that these decay channels almost saturate the decay of the hybrid mesons, since contributions from decay channels such as an S-wave $q\bar{q}$ meson plus a P-wave one and a hybrid meson (or glueball) plus a $q\bar{q}$ meson and from the direct multibody decays will be small (or kinematically forbidden) because of low mass of the initial hybrid mesons. We will use the experimental width of the $f_1(1420)$ as input to fix the absolute scale of the coupling strength g. As for the value of the magnetic coupling, we use $h_M=1.69$ obtained from the analysis [17] of the spin-spin splitting of $q\bar{q}$ mesons.

B. Effective Hamiltonians for respective decay processes

The effective Hamiltonians in momentum space for our relevant respective decay processes are systematically obtained from Eq. (3.1). The only necessary work is to substitute the following decompositions of our multilocal fields into Eq. (3.1) and to perform the space-time integration.

Separating the plane wave functions for the center-of-mass motion as

$$H_{\alpha,\nu}^\beta(X_H,\rho,\lambda;P_H)=\frac{e^{iP_H\cdot X_H}}{[(2\pi)^3 2E_H]^{1/2}}\Psi_{H\alpha,\nu}^\beta(\rho,\lambda;P_H)\ , \tag{3.4a}$$

$$\Phi_\alpha^\beta(X_i,x_i;P_i)=\frac{e^{iP_i\cdot X_i}}{[(2\pi)^3 2E_i]^{1/2}}\Psi_\alpha^\beta(x_i;P_i)\quad(i=B,C)\ , \tag{3.4b}$$

the internal wave functions $\Psi_{H\alpha,\nu}^\beta(\rho,\lambda;P_H)$ and $\Psi_\alpha^\beta(x_i;P_i)$ are written, respectively, as

$$\Psi_{H\alpha,\nu}^\beta(\rho,\lambda;P_H)=\frac{1}{2\sqrt{2}}\left[\gamma_5\left[1+\frac{i\gamma\cdot P_H}{M_H}\right]\right]_\alpha^\beta H_\nu(P_H)\psi_H(\rho,\lambda;P_H)+\frac{1}{2\sqrt{2}}\left[\gamma_\mu\left[1+\frac{i\gamma\cdot P_H}{M_H}\right]\right]_\alpha^\beta H_{\mu\nu}(P_H)\psi_H(\rho,\lambda;P_H)\ , \tag{3.5a}$$

with

$$\psi_H(\rho,\lambda;P_H)=\frac{\alpha_\rho\alpha_\lambda}{\pi^2}\exp\left[-\frac{\alpha_\rho}{2}\left\{\rho^2+2\frac{(P_H\cdot\rho)^2}{M_H^2}\right\}-\frac{\alpha_\lambda}{2}\left\{\lambda^2+2\frac{(P_H\cdot\lambda)^2}{M_H^2}\right\}\right] \tag{3.5b}$$

and

$$\Psi_\alpha^\beta(x_i;P_i)=\frac{1}{2\sqrt{2}}\left[\gamma_5\left[1+\frac{i\gamma\cdot P_i}{M_i}\right]\right]_\alpha^\beta P(P_i)\psi_i(x_i;P_i)+\frac{1}{2\sqrt{2}}\left[\gamma_\mu\left[1+\frac{i\gamma\cdot P_i}{M_i}\right]\right]_\alpha^\beta V_\mu(P_i)\psi_i(x_i;P_i)\ , \tag{3.6a}$$

with

$$\psi_i(x_i;P_i)=\frac{\beta_i}{\pi}\exp\left[-\frac{\beta_i}{2}\left\{x_i^2+2\frac{(P_i\cdot x_i)^2}{M_i^2}\right\}\right]\ , \tag{3.6b}$$

where the explicit form of the internal space-time wave function $\psi(\rho,\lambda;P_H)$ [$\psi_i(x_i;P_i)$] for initial hybrid [final ordinary] mesons has been determined from Eqs. (2.7) and (2.8) (the equations similar to those [11,17] given in previous work); $H_\nu(P_H)$ and $H_{\mu\nu}(P_H)$ may be treated as ordinary local fields describing our ground-state hybrid mesons with the quark-spin configurations $S=0$ and 1, and similarly $P(P_i)$ and $V_\mu(P_i)$ are the local field representing pseudoscalar and vector mesons, respectively. Concerning the four-vector indices μ and ν, these "local" fields satisfy, because of Eqs. (2.2) and (2.3) and because of the equations similar [10] to Eq. (2.2) for $V_\mu(P_i)$, the constraints

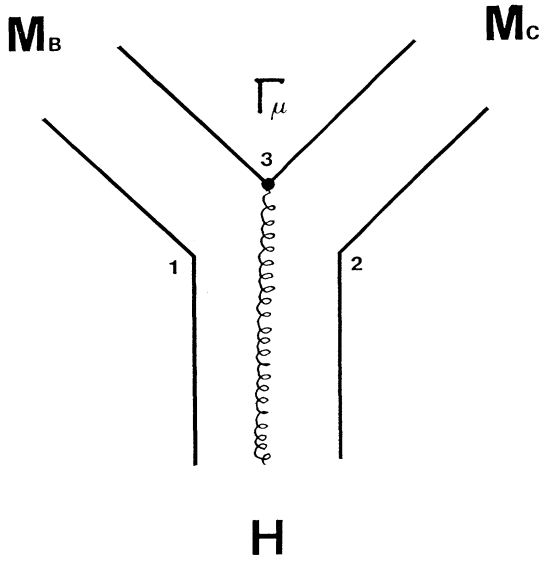

FIG. 1. Decay mechanism of hybrid mesons into two ordinary mesons.

$$P_{H\mu}H_{\mu}(P_H)=0\ ,\quad P_{H\mu}H_{\mu\nu}(P_H)=P_{H\nu}H_{\mu\nu}(P_H)=0 \tag{3.7a}$$

and

$$P_{i\mu}V_{\mu}(P_i)=0\ , \tag{3.7b}$$

where the "local" field $H_{\mu}(P_H)$ represents axial-vector mesons with $J^{PC}=1^{+-}$, while the "local" field $H_{\mu\nu}(P_H)$ is decomposed into scalar, axial-vector, and tensor mesons with $J^{PC}=0^{++}$, 1^{++}, and 2^{++}, respectively, satisfying the subsidiary conditions

$$H_{\mu\nu}(P_H)=H_{\nu\mu}(P_H)\ ,\quad H_{\mu\mu}(P_H)\neq 0$$

for scalar mesons ,

$$H_{\mu\nu}(P_H)=-H_{\nu\mu}(P_H)\quad \text{for axial-vector mesons}\ , \tag{3.8}$$

$$H_{\mu\nu}(P_H)=H_{\nu\mu}(P_H)\ ,\quad H_{\mu\mu}(P_H)=0$$

for tensor mesons .

The various constants appearing in Eqs. (3.4)–(3.6) are expressed in terms of the fundamental model parameters of the effective quark and gluon masses and the potential strength K as

$$\alpha_{\rho}=\frac{\sqrt{7}}{16}\sqrt{32mK}\ ,$$
$$\alpha_{\lambda}=\frac{9}{16}\left[\frac{m_g}{2m+m_g}\right]^{1/2}\sqrt{32mK}\ , \tag{3.9}$$
$$\beta_i=\frac{\sqrt{2}}{8}\left[\frac{m_p}{m+m_p}\right]^{1/2}\sqrt{32mK}\ ,$$

and M_H (M_i) is "symmetric" mass of hybrid (ordinary) mesons given by Eq. (2.13a) (the equation similar to that [17] given in previous work). Here m_p represents the effective mass of a quark (antiquark) converted from the gluon. It is to be noted that in the equations throughout this section the center-of-mass momenta of mesons P_{μ} are "symmetric" ones (denoted by capital letters), satisfying $P_{\mu}^2=-M^2$ for respective mesons.

The effective Hamiltonians for respective decay processes thus obtained are collected in Table IV. All the effective coupling constants in this table are written in terms of g, h_M, K, m_q, m_g, M_H, and M_i, expressions of which are given in Appendix B. In the effective "local" interactions in Table IV, the center-of-mass momenta of mesons are treated as physical ones (denoted by small letters), satisfying $p_{\mu}^2=-m^2$ for respective mesons, in order to take account of the effects of phase space correctly. The value of g is taken to be 6.6 GeV determined from the experimental width of $\Gamma\ [f_1(1420)\rightarrow K^*\bar{K}]\approx 55$ MeV, as mentioned above. The used values for other parameters are also given in Appendix B.

C. Decay widths of the ground-state hybrid mesons

From the effective Hamiltonians given in Table IV, the partial decay widths for respective processes are directly obtained following the ordinary procedure. All the formulas for the partial decay widths thus obtained are collected in Table V. By using the effective coupling constants fixed as explained in the last subsection, we obtain the numerical values for the partial decay widths and for the total decay widths as a sum of the former ones. All the results are given in Table VI, where we have shown the respective widths for the two limiting cases of taking lower and upper mass values for the ground-state hybrid mesons within the mass range discussed in Sec. II B.

From this table we see that our theoretical decay widths for the respective hybrid-meson nonets with J^{PC} have the following characteristic features.

1^{+-} *nonet.* All members have a narrow width of less than about 100 MeV, except for h_{g1} with $\Gamma\approx 150$–220 MeV.

0^{++} *nonet.* All members have a narrow width of less than 100 MeV, except for f_{g0} with $\Gamma\approx 130$–150 MeV, in contrast with the corresponding $q\bar{q}$ states, which are expected generally to have a very broad width of several hundred MeV.

1^{++} *nonet.* All members have a very broad width of more than about 400–500 MeV, except for the $f_{g1}(1420)$, which is our "input" hybrid meson. This is due to the fact that generally this nonet couples strongly with the PV channel [P (V) stands for pseudoscalar (vector) mesons], while the $f_{g1}(1420)$ has very small threshold energy for its dominant decay channel $K^*\bar{K}$.

2^{++} *nonet.* Each member of this nonet has a width of about 100–300 MeV, depending upon its mass, which is moderate for observation, and they couple strongly with the VV and/or PV channels, while very weakly with the PP channel.

Thus we can understand why only the $f_{g1}(1420)$ has been observed out of the members of the 1^{++} nonet, and we see that there is a good chance for observing the

members of the 1^{+-}, 0^{++}, and 2^{++} nonets, which generally have a moderate width for their observation. Here it may be worthwhile to note that the above features are related to the "rest rule" concerning the overlapping of our relativistic spin wave function at zero threshold energy.

IV. EXPERIMENTAL CANDIDATES FOR HYBRID MESONS

A. General remarks on searching for hybrid mesons

In our scheme the ground-state hybrid mesons have the same quantum numbers as the P-wave $q\bar{q}$ mesons and both are expected to have similar masses, as was discussed in Sec. II B. We called this fact the "doubling" between these two meson states. So, in order to identify hybrid mesons, discriminating from $q\bar{q}$ mesons or generally from the other mesons, it is necessary to make deliberate physical considerations from various viewpoints.

Since hybrid mesons contain an extra gluon compared to $q\bar{q}$ mesons, they are expected to be produced more abundantly in gluon-rich processes such as the diffractive process (where the production mechanism is dominated by Pomeron exchange, which is considered [18] to be multigluon exchange in QCD) and the central-collision process (where double Pomeron or Pomeron-Reggeon exchange are dominant), while these processes contain generally strong background effects (especially in the diffractive process of the Drell-Hiida-Deck effect [19]). On the other hand, they are expected to be less abundantly produced in peripheral-collision processes such as the charge-exchange reaction (being dominated by an ordinary $q\bar{q}$-meson pole), while these processes may be comparatively "clean."

There are other interesting production processes for hybrid mesons: two-photon collisions, through which our first hybrid meson $f_1(1420)$ has been observed [20]. J/ψ decays into hadrons and into hadrons plus a photon, where the $f_1(1420)$ also has been observed [21], which are Okubo-Zweig-Iizuka- (OZI-) forbidden processes and

TABLE IV. Effective Hamiltonians for the ground-state hybrid mesons decaying into two ordinary S-wave $q\bar{q}$ mesons. The expression of the effective coupling constants in terms of the fundamental model parameters are given in Appendix B.

Decay process[a]	Effective Hamiltonian
$B\to V+P$	$g^{(1)}_{BVP}H_\nu(p_H)V_\nu(p_B)P(p_C)$
	$+g^{(2)}_{BVP}p_{C\nu}H_\nu(p_H)p_{C\tau}V_\tau(p_B)P(p_C)$
$B\to V+V$	$ig^{(1)}_{BVV}\epsilon_{\tau\sigma\nu\alpha}p_{B\alpha}H_\nu(p_H)V_\tau(p_B)V_\sigma(p_C)$
	$+ig^{(2)}_{BVV}\epsilon_{\tau\sigma\nu\alpha}p_{C\alpha}H_\nu(p_H)V_\tau(p_B)V_\sigma(p_C)$
	$+ig^{(3)}_{BVV}\epsilon_{\tau\nu\alpha\beta}p_{B\alpha}p_{C\beta}p_{B\sigma}H_\nu(p_H)V_\tau(p_B)V_\sigma(p_C)$
	$+ig^{(4)}_{BVV}\epsilon_{\tau\sigma\alpha\beta}p_{B\alpha}p_{C\beta}p_{B\nu}H_\nu(p_H)V_\tau(p_B)V_\sigma(p_C)$
	$+ig^{(5)}_{BVV}\epsilon_{\sigma\nu\alpha\beta}p_{B\alpha}p_{C\beta}H_\nu(p_H)p_{C\tau}V_\tau(p_B)V_\sigma(p_C)$
$S\to P+P$	$g^{(1)}_{SPP}H_{\mu\mu}(p_H)P(p_B)P(p_C)$
	$+g^{(2)}_{SPP}p_{B\mu}p_{B\nu}H_{\mu\nu}(p_H)P(p_B)P(p_C)$
$S\to V+V$	$g^{(1)}_{SVV}H_{\mu\nu}(p_H)V_\mu(p_B)V_\nu(p_C)$
	$+g^{(2)}_{SVV}p_{B\nu}H_{\mu\nu}(p_H)V_\mu(p_B)p_{B\sigma}V_\sigma(p_C)$
	$+g^{(3)}_{SVV}p_{C\nu}H_{\mu\nu}(p_H)p_{C\tau}V_\tau(p_B)V_\mu(p_C)$
	$+g^{(4)}_{SVV}p_{B\mu}p_{B\nu}H_{\mu\nu}(p_H)V_\tau(p_B)V_\tau(p_C)$
	$+g^{(5)}_{SVV}p_{B\mu}p_{B\nu}H_{\mu\nu}(p_H)p_{C\tau}V_\tau(p_B)p_{B\sigma}V_\sigma(p_C)$
$A\to V+P$	$ig^{(1)}_{AVP}\epsilon_{\tau\mu\nu\alpha}p_{H\alpha}H_{\mu\nu}(p_H)V_\tau(p_B)P(p_C)$
	$+ig^{(2)}_{AVP}\epsilon_{\tau\mu\nu\alpha}p_{B\alpha}H_{\mu\nu}(p_H)V_\tau(p_B)P(p_C)$
	$+ig^{(3)}_{AVP}\epsilon_{\tau\mu\alpha\beta}p_{H\alpha}p_{B\beta}p_{B\nu}H_{\mu\nu}(p_H)V_\tau(p_B)P(p_C)$
	$+ig^{(4)}_{AVP}\epsilon_{\alpha\beta\mu\nu}p_{H\alpha}p_{C\beta}H_{\mu\nu}(p_H)p_{C\tau}V_\tau(p_B)P(p_C)$
$A\to V+V$	$g^{(1)}_{AVV}p_{B\nu}H_{\mu\nu}(p_H)V_\mu(p_B)p_{B\sigma}V_\sigma(p_C)$
	$+g^{(2)}_{AVV}p_{B\nu}H_{\mu\nu}(p_H)p_{C\tau}V_\tau(p_B)V_\mu(p_C)$
$T\to P+P$	$g^{(1)}_{TPP}p_{B\mu}p_{B\nu}H_{\mu\nu}(p_H)P(p_B)P(p_C)$
$T\to V+P$	$g^{(1)}_{TVP}\epsilon_{\tau\mu\alpha\beta}p_{H\alpha}p_{B\beta}p_{B\nu}H_{\mu\nu}(p_H)V_\tau(p_B)P(p_C)$
$T\to V+V$	$g^{(1)}_{TVV}H_{\mu\nu}(p_H)V_\mu(p_B)V_\nu(p_C)$
	$+g^{(2)}_{TVV}p_{B\mu}p_{B\nu}H_{\mu\nu}(p_H)V_\tau(p_B)V_\tau(p_C)$
	$+g^{(3)}_{TVV}p_{B\nu}H_{\mu\nu}(p_H)V_\mu(p_B)p_{H\sigma}V_\sigma(p_C)$
	$+g^{(4)}_{TVV}p_{B\nu}H_{\mu\nu}(p_H)p_{H\tau}V_\tau(p_B)V_\mu(p_C)$
	$+g^{(5)}_{TVV}p_{B\mu}p_{B\nu}H_{\mu\nu}(p_H)p_{H\tau}V_\tau(p_B)p_{H\sigma}V_\sigma(p_C)$

[a] B, S, A, and T represent hybrid mesons, respectively, with $J^{PC}=1^{+-}$, 0^{++}, 1^{++}, and 2^{++} and P (V) S-wave $q\bar{q}$ mesons with $J^{PC}=0^{-+}$ (1^{--}).

TABLE V. Decay width formulas for the ground-state hybrid mesons decaying into two ordinary $q\bar{q}$ mesons. The decay widths are given by

$$\Gamma=\frac{1}{8\pi}\frac{|\mathbf{p}|}{m_H^2}\frac{1}{2J+1}\sum_{\text{spin}}|\mathcal{M}|^2 ,$$

where $|\mathbf{p}|=[\{m_H^2-(m_B+m_C)^2\}\{m_H^2-(m_B-m_C)^2\}]^{1/2}/2m_H$ and m_H (m_B and m_C) is real mass of initial hybrid (final $q\bar{q}$) mesons. The effective coupling constants g_i for each process are given in Appendix B. (Note that the subscripts of the coupling constants indicating decay processes are omitted in the table.)

Decay process	$\frac{1}{2J+1}\sum_{\text{spin}}\lvert\mathcal{M}\rvert^2$
$B\to V+P$	$g_1^2\left[3+\frac{\mathbf{p}^2}{m_B^2}\right]+2g_1g_2\left[1-\frac{(p_Bp_C)}{m_B^2}\mathbf{p}^2\right]+g_2^2\frac{m_H^2}{m_B^2}\mathbf{p}^4$
$B\to V+V$	$6\left[(g_1E_B+g_2E_C)^2+\left\{\frac{g_1-g_2}{E_B}+g_5m_H\left[1+\frac{E_C}{E_B}\right]\right\}^2\mathbf{p}^4+\left\{\frac{g_1-g_2}{E_C}-g_3m_H\left[1+\frac{E_B}{E_C}\right]\right\}^2\mathbf{p}^4+g_4^2m_H^2\right]$
	$+4\left[-(g_1E_B+g_2E_C)\left\{\frac{g_1-g_2}{E_B}+g_5m_H\left[1+\frac{E_C}{E_B}\right]\right\}\right.$
	$\left.+(g_1E_B+g_2E_C)g_4m_H+(g_1E_B+g_2E_C)\left\{\frac{g_1-g_2}{E_C}-g_3m_H\left[1+\frac{E_B}{E_C}\right]\right\}\right]\mathbf{p}^2$
	$+4\left[\left\{\frac{g_1-g_2}{E_B}+g_5m_H\left[1+\frac{E_C}{E_B}\right]\right\}g_4m_H+\left\{\frac{g_1-g_2}{E_B}+g_5m_H\left[1+\frac{E_C}{E_B}\right]\right\}\left\{\frac{g_1-g_2}{E_C}-g_3m_H\left[1+\frac{E_B}{E_C}\right]\right\}\right.$
	$\left.-\left\{\frac{g_1-g_2}{E_C}-g_3m_H\left[1+\frac{E_B}{E_C}\right]\right\}g_4m_H\right]\mathbf{p}^4$
	$+\frac{2}{m_B^2}\left[(g_1E_B+g_2E_C)-\left\{\frac{g_1-g_2}{E_B}+g_5m_H\left[1+\frac{E_C}{E_B}\right]\right\}\mathbf{p}^2\right]^2\mathbf{p}^2$
	$+\frac{2}{m_C^2}\left[(g_1E_B+g_2E_C)-\left\{\frac{g_1-g_2}{E_C}-g_3m_H\left[1+\frac{E_B}{E_C}\right]\right\}\mathbf{p}^2\right]^2\mathbf{p}^2$
$S\to P+P$	$9g_1^2+6g_1g_2|\mathbf{p}|+g_2^2\mathbf{p}^2$
$S\to V+V$	$\frac{1}{3}\left[g_1^2\left[2+\frac{(p_Bp_C)^2}{m_B^2m_C^2}\right]+g_2^2\left[m_Bm_C-\frac{(p_Bp_C)^2}{m_Bm_C}\right]^2+g_3^2\left[3+\frac{\mathbf{p}^2}{m_B^2}+\frac{\mathbf{p}^2}{m_C^2}+\frac{\mathbf{p}^4}{m_B^2m_C^2}\right]\right.$
	$+g_4^2\left[1+\frac{\mathbf{p}^2}{m_B^2}\right]\left[\frac{(p_Bp_C)^2}{m_B^2}-m_B^2\right]+g_5^2\left[1+\frac{\mathbf{p}^2}{m_C^2}\right]\left[\frac{(p_Bp_C)^2}{m_C^2}-m_C^2\right]+2g_1g_2(p_Bp_C)\left[-1+\frac{(p_Bp_C)^2}{m_B^2m_C^2}\right]$
	$+2g_1g_5\frac{(p_Bp_C)\mathbf{p}^2}{m_B^2}\left[1-\frac{(p_Bp_C)}{m_C^2}\right]+2g_1g_3\left[3+\frac{\mathbf{p}^2}{m_B^2}+\frac{\mathbf{p}^2}{m_C^2}-\frac{\mathbf{p}^2(p_Bp_C)}{m_B^2m_C^2}\right]-2g_1g_4\frac{(p_Bp_C)\mathbf{p}^2}{m_C^2}\left[1-\frac{(p_Bp_C)}{m_B^2}\right]$
	$-2g_2g_3\left[1-\frac{(p_Bp_C)}{m_B^2}\right]\left[1-\frac{(p_Bp_C)}{m_C^2}\right]\mathbf{p}^2+2g_2g_4(m_B^2-(p_Bp_C))\left[1-\frac{(p_Bp_C)^2}{m_B^2m_C^2}\right]\mathbf{p}^2$
	$-2g_2g_5(m_C^2-(p_Bp_C))\left[1-\frac{(p_Bp_C)^2}{m_B^2m_C^2}\right]\mathbf{p}^2-2g_3g_5\left[1+\frac{\mathbf{p}^2}{m_C^2}\right]\left[1-\frac{(p_Bp_C)}{m_B^2}\right]\mathbf{p}^2$
	$\left.-2g_4g_5\left[1-\frac{(p_Bp_C)}{m_B^2}\right]\left[1-\frac{(p_Bp_C)}{m_C^2}\right]\mathbf{p}^4\right]$
$A\to V+P$	$\frac{1}{3}g_3^2m_H^2\mathbf{p}^4+\frac{2}{3}\left[g_4m_H+\frac{g_2}{E_B}\right]^2\left[1+\frac{\mathbf{p}^2}{m_B^2}\right]\mathbf{p}^4-\frac{4}{3}\left[g_4m_H+\frac{g_2}{E_B}\right](g_1m_H+g_2E_B)\left[1+\frac{\mathbf{p}^2}{m_B^2}\right]\mathbf{p}^2$
	$+\frac{2}{3}(g_1m_H+g_2E_B)^2\left[3+\frac{\mathbf{p}^2}{m_B^2}\right]-\frac{4}{3}g_3m_H(g_1m_H+g_2E_B)\mathbf{p}^2$
$A\to V+V$	$\frac{1}{3}\left[\frac{g_1^2}{m_C^2}+\frac{g_2^2}{m_B^2}\right]m_H^2\mathbf{p}^4$
$T\to P+P$	$\frac{2}{15}g^2\mathbf{p}^4$
$T\to V+P$	$\frac{1}{5}g^2m_H^2\mathbf{p}^4$

TABLE V. (*Continued*).

Decay process	$\frac{1}{2J+1}\sum_{\text{spin}}\lvert\mathcal{M}\rvert^2$
$T\to V+V$	$\frac{1}{15}\left[g_1^2\left[9+10\frac{\mathbf{p}^2}{m_B^2}+10\frac{\mathbf{p}^2}{m_C^2}+2\frac{\mathbf{p}^4}{m_B^2m_C^2}\right]+4g_2^2\left[1+\frac{(p_Bp_C)^2}{m_B^2m_C^2}\right]\mathbf{p}^4+g_3^2\left[-5m_H^2\mathbf{p}^2+5\frac{(p_Cp_H)^2}{m_C^2}\mathbf{p}^2-2\frac{m_H^2}{m_B^2}\mathbf{p}^4\right.\right.$ $\left.+2\frac{(p_Cp_H)^2}{m_B^2m_C^2}\mathbf{p}^4\right]+g_4^2\left[-5m_H^2\mathbf{p}^2+5\frac{(p_Bp_H)^2}{m_B^2}\mathbf{p}^2-2\frac{m_H^2}{m_C^2}\mathbf{p}^4+2\frac{(p_Bp_H)^2}{m_B^2m_C^2}\mathbf{p}^4\right]$ $+4g_5^2\left[m_H^4-m_H^2\frac{(p_Cp_H)^2}{m_C^2}-m_H^2\frac{(p_Bp_H)^2}{m_B^2}+\frac{(p_Bp_H)^2(p_Cp_H)^2}{m_B^2m_C^2}\right]\mathbf{p}^4+4g_1g_2\left[\frac{\mathbf{p}^4}{m_C^2}+\frac{\mathbf{p}^4}{m_B^2}-\frac{(p_Bp_C)}{m_B^2m_C^2}\mathbf{p}^4\right]$ $-2g_1g_3\left[5\frac{(p_Cp_H)}{m_C^2}\mathbf{p}^2+2\frac{(p_Cp_H)}{m_B^2m_C^2}\mathbf{p}^4\right]+2g_1g_4\left[5\frac{(p_Bp_H)}{m_B^2}\mathbf{p}^2+2\frac{(p_Bp_H)}{m_B^2m_C^2}\mathbf{p}^4\right]-4g_1g_5\frac{(p_Bp_H)(p_Cp_H)}{m_B^2m_C^2}\mathbf{p}^4$ $+4g_2g_3\left[-\frac{(p_Cp_H)}{m_C^2}+\frac{(p_Bp_H)}{m_B^2}+\frac{(p_Bp_C)(p_Cp_H)}{m_B^2m_C^2}\right]\mathbf{p}^4+4g_2g_4\left[-\frac{(p_Cp_H)}{m_C^2}+\frac{(p_Bp_H)}{m_B^2}-\frac{(p_Bp_C)(p_Bp_H)}{m_B^2m_C^2}\right]\mathbf{p}^4$ $+4g_2g_5\left[m_H^2+\frac{(p_Cp_H)^2}{m_C^2}+\frac{(p_Bp_H)^2}{m_B^2}+\frac{(p_Bp_C)(p_Bp_H)(p_Cp_H)}{m_B^2m_C^2}\right]\mathbf{p}^4$ $-4g_3g_4\frac{(p_Bp_H)(p_Cp_H)}{m_B^2m_C^2}\mathbf{p}^4+4g_3g_5\left[\frac{m_H^2(p_Bp_H)}{m_B^2}+\frac{(p_Bp_H)(p_Cp_H)^2}{m_B^2m_C^2}\right]\mathbf{p}^4$ $\left.+4g_4g_5\left[\frac{m_H^2(p_Cp_H)}{m_C^2}-\frac{(p_Bp_H)^2(p_Cp_H)}{m_B^2m_C^2}\right]\mathbf{p}^4\right]$

TABLE VI. Predicted partial and total decay widths of the ground-state hybrid mesons. The isoscalar mixings for hybrid mesons are simply taken to be ideal in each nonet, that is, f_g, $h_g=(u\bar{u}+d\bar{d})g/\sqrt{2}$ and f_g', $h_g'=-s\bar{s}g$. The singlet-octet mixing angle for the η and η' mesons is taken to be $-20°$.

$^{2S+1,2\Sigma+1}L_J$[a]	I^GJ^{PC}	Hybrid meson[b] mass (MeV)	Decay modes	Partial width (MeV)	Total width (MeV)
$^{13}S_1$	1^+1^{+-}	b_{g1}	$\omega\pi$	48–56	
		1300–1500	$\rho\eta$	13–21	61–91
			$\phi\pi$	0	
			$K^*\bar{K}$	0–14	
	$\frac{1}{2}1^+$	$K_{g1}^{(B)}$	$K^*\pi$	0–30	
		1400–1600	$K^*\eta$	≈ 0	
			ρK	22–32	29–81
			ωK	7–10	
			ϕK	0–9	
	0^-1^{+-}	h_{g1}	$\rho\pi$	150–170	
		1300–1500	$\omega\eta$	0–20	150–220
			$K^*\bar{K}$	0–28	
		h_{g1}'	$\rho\pi$	0	
		1550–1750	$\omega\eta$	0	50–87
			$\phi\eta$	0–16	
			$K^*\bar{K}$	50–71	
$^{31}S_0$	1^-0^{++}	a_{g0}	$\eta\pi$	38–41	
		1200–1400	$\eta'\pi$	8–11	78–82
			$K\bar{K}$	28–30	
	$\frac{1}{2}0^+$	K_{g0}^*	$K\pi$	41–46	
		1300–1500	$K\eta$	≈ 0	41–58
			$K\eta'$	0–12	

TABLE VI. (*Continued*).

$^{2S+1,2\Sigma+1}L_J$[a]	I^GJ^{PC}	Hybrid meson[b] mass (MeV)	Decay modes	Partial width (MeV)	Total width (MeV)
$^{31}S_0$	0^+0^{++}	f_{g0}	$\pi\pi$	98–114	
		1200–1400	$\eta\eta$	7–10	130–150
			$K\bar{K}$	27–30	
		f'_{g0}	$\pi\pi$	0	
		1450–1650	$\eta\eta$	0–5	
			$\eta\eta'$	0–11	
			$K\bar{K}$	44–46	44–62
			$\rho\rho$	0	
			$\omega\omega$	0	
$^{33}S_1$	1^-1^{++}	a_{g1}	$\rho\pi$	600–840	
		1300–1500	$K^*\bar{K}$	0–94	600–930
	$\frac{1}{2}1^+$	K^A_{g1}	$K^*\pi$	220–300	
		1400–1600	$K^*\eta$	0–160	
			ρK	160–260	430–900
			ωK	51–84	
			ϕK	0–93	
	0^+1^{++}	$f_{g1}(1420)$	$K^*\bar{K}$	55 (input)	55
		1420			
		f'_{g1}	$K^*\bar{K}$	290–430	
		1550–1750	$\rho\rho$	0	290–430
			$\omega\omega$	0	
$^{35}S_2$	1^-2^{++}	a_{g2}	$\eta\pi$	1–2	
		1400–1600	$\eta'\pi$	≈ 0	
			$K\bar{K}$	≈ 0	
			$\rho\pi$	93–310	94–370
			$K^*\bar{K}$	0–13	
			$\rho\omega$	0–48	
	$\frac{1}{2}2^+$	K^*_{g2}	$K\pi$	2–3	
		1500–1700	$K\eta$	≈ 0	
			$K\eta'$	≈ 0	
			$K^*\pi$	33–120	
			$K^*\eta$	0–21	
			ρK	14–80	53–290
			ωK	4–25	
			ϕK	0–6	
			$K^*\rho$	0–30	
			$K^*\omega$	0–8	
	0^+2^{++}	f_{g2}	$\pi\pi$	5–7	
		1400–1600	$\eta\eta$	0–7	
			$\eta\eta'$	≈ 0	
			$K\bar{K}$	≈ 0	
			$K^*\bar{K}$	0–13	12–120
			$\rho\rho$	0–82	
			$\omega\omega$	0–21	
		f'_{g2}	$\pi\pi$	0	
		1650–1850	$\eta\eta$	≈ 0	
			$\eta\eta'$	≈ 0	
			$K\bar{K}$	≈ 1	
			$K^*\bar{K}$	25–130	26–170
			$\rho\rho$	0	
			$\omega\omega$	0	
			$K^*\bar{K}^*$	0–42	

[a] $S=S_q+S_{\bar{q}}$, $\Sigma=S+S_g$, $L=L_\rho+L_\lambda$, and $J=L+\Sigma$.

[b] The symbols for hybrid mesons conform to the standard naming scheme for ordinary $q\bar{q}$ mesons except for the subscript g indicating an extra gluon as a constituent.

accordingly are comparatively gluon rich. These collision and decay processes are also clean. The Primakov process [22], where the concerned dynamics is well known, QED, and hybrid mesons may be expected [23] to be produced as much as ordinary $q\bar{q}$ mesons.

Here it is worthwhile to stress the importance of the interference effect between the two doubling states. Since these two states with the same quantum numbers have generally different particle properties, a "single" (thus far considered) resonance may have a different mass and width depending upon its production processes and decay channels due to the interference effect. Actually, we have shown in a separate paper [24] the possibility that the puzzle of the "variant mass and width" of the axial-vector a_1 meson is solved by this effect (see a discussion on the 1^{++} nonet in the following subsection).

B. Candidates for the ground-state hybrid mesons

Now, by making use of our predicted decay properties of the ground-state hybrid mesons given in Table VI and their characteristic features discussed in Sec. III C, we try to select several possible candidates [other than the $f_1(1420)$] for the respective members of their four nonets out of still-unclassified observed mesons listed in Table II. The candidates are collected in Table VII, where our theoretical total decay widths and branching ratios (for their "observed" masses) are given in comparison with the present experimental properties.

We give some comments on their candidates assigned to each nonet with J^{PC} in the following.

1^{+-} nonet. There exist respective candidates for the two members b_{g1} and $K_{g1}^{(B)}$. In the recent experiment at KEK on the charge-exchange reaction $\pi^- p \to M^0 n$, they have observed [25–27] a peak both in the $\omega\pi^0$ and $\rho\eta$ channels. The respective peaks have the same quantum numbers $(I^G, J^{PC}) = (1^+, 1^{+-})$ as those of the b_1 meson, while their masses and widths seem to be very different with each other. The mass and width for a peak in the $\omega\pi^0$ channel were $m = 1236 \pm 16$ MeV and $\Gamma = 151 \pm 31$ MeV [25], which are consistent with the world averages [28] of the $b_1(q\bar{q})$ meson. On the other hand, those for a peak in the $\rho\eta$ channel were $m = 1311 \pm 10$ MeV and $\Gamma = 126 \pm 10$ MeV [26], which are higher and narrower, respectively. A similar inclination has been seen [29] in the "b_1 meson" observed through the $\rho\eta$ channel by the Omega Photon Collaboration.

Recently, we have shown [24] that both spectra in the $\omega\pi$ and $\rho\eta$ channels are well reproduced by the interference effect between the two doubling states b_1 and b_{g1}.

TABLE VII. Predicted decay properties of the candidates for the ground-state hybrid mesons in comparison with experiment. The singlet-octet mixing angle for the η and η' mesons is taken to be $-20°$ in the prediction.

Meson	Experiment[a]			Prediction		
mass (MeV)	Total width (MeV)	Observed channel	Assignment	Total width (MeV)	Decay modes	Branching fraction (%)
$b_1(1300)$	≈ 50	$\eta(\pi\pi)_\rho$	$b_{g1}(1300)$	55	$\omega\pi$	88
≈ 1300					$\rho\eta$	12
$K_1(1650)$	150 ± 50	ϕK	$K_{g1}^{(B)}(1650)$	180	$K^*\pi$	40
1650 ± 50					ρK	37
					ωK	12
					ϕK	11
					$K^*\eta$	≈ 0
$a_0(1320)$	130 ± 30	$\eta\pi$	$a_{g0}(1320)$	78	$\eta\pi$	50
1322 ± 30					$\eta'\pi$	13
					$K\bar{K}$	37
$f_0(1240)$	140 ± 10	$K\bar{K}$	$f_{g0}(1240)$	150	$\pi\pi$	75
1240 ± 10					$K\bar{K}$	19
					$\eta\eta$	6
$f_0(1525)$	≈ 90	$K\bar{K}$	$f'_{g0}(1525)$	54	$K\bar{K}$	84
≈ 1525					$\eta\eta$	9
					$\eta\eta'$	7
					$\pi\pi$	0
$a_1(1400)$	≈ 700	$\rho\pi$	$a_{g1}(1400)$	740	$\rho\pi$	95
≈ 1400					$K^*\bar{K}$	5
$f_1(1420)$	55 ± 3	$K^*\bar{K}$	$f_{g1}(1420)$	55 (input)	$K^*\bar{K}$	≈ 100
1425.3 ± 1.3						
$f_2(1640)$	< 70	$\omega\omega$	$f_{g2}(1640)$	160	$\rho\rho$	64
1635 ± 7					$\omega\omega$	18
					K^*K	13
					$\pi\pi$	5
					$\eta\eta$	≈ 0
					$\eta\eta'$	≈ 0
					$K\bar{K}$	≈ 0

[a]The data are taken from Ref. [28] except for the $b_1(1300)$ and $a_1(1400)$. For these two mesons, see discussions in Sec. IV B.

We have given the mass and width of b_{g1} used through this analysis in Table VII. It is to be noted that the values of (mass and) width for the b_{g1} meson are our predicted ones.

The candidate $K_1(1650)$ for $K_{g1}^{(B)}$ selected in Table VII has a similar mass and total decay width to our prediction, but is observed in the ϕK channel. It is important to confirm it in our predicted main channels $K^*\pi$ and ρK.

Here we would like to point out that some structures in the mass region of 1.3–1.5 GeV have been seen [30] in the $\rho\pi$ channel in the same KEK experiment, which might be due to h_{g1}. An experimental analysis of the $\omega\eta$ channel is interesting in confirmation of existence of h_{g1} if its mass is large enough to decay into this channel, although its coupling is rather small. In this channel with high threshold energy, the influence of the $h_1(q\bar{q})$ and $h_1'(q\bar{q})$, which have a lower mass, upon the observed spectrum of h_{g1} is expected to be small.

1^{++} *nonet.* There exist respective candidates for the two members f_{g1} and a_{g1}. The $f_1(1420)$ is our "input" hybrid meson f_{g1}.

In the recent experiment at KEK on the peripheral charge-exchange reaction $\pi^- p \to M^0 n$, they observed [30] a peak in the $\rho\pi$ channel with the same quantum number $(I^G, J^{PC}) = (1^-, 1^{++})$ as the a_1 meson. Its mass and width are 1122 ± 17 and 254 ± 11 MeV, respectively, which are very different from the values of $m = 1280\pm30$ MeV and $\Gamma = 300\pm50$ MeV thus far obtained [31] in the diffractive process and also from $m = 1208\pm15$ MeV and $\Gamma = 430\pm50$ MeV recently obtained [32] in the central production process, while its mass value is close to the one simply obtained [33] in the τ decay without any complex manipulations but its width is much narrower.

This "puzzle" [34] is interpreted as being also due to the interference effect between the two doubling states a_1 and a_{g1}. In the "gluon-poor" peripheral charge-exchange and τ-decay processes, the a_1 meson is considered to be produced more abundantly than the a_{g1}, while in the "gluon-rich" diffractive and central-collision processes it is vice versa. Actually, we have shown [24] that both "a_1 spectra" in the peripheral charge-exchange and central-collision experiments are well reproduced phenomenologically as superposed decay spectra of the doubling states of a_1 and a_{g1}. The mass and width of a_{g1} used through this analysis are given in Table VII. It is to be noted that the broad a_{g1} width of about 700 MeV is our predicted value, while its mass of about 1400 MeV is rather appropriately chosen.

0^{++} *nonet.* There exist respective candidates for the three members a_{g0}, f_{g0}, and f_{g0}' as shown in Table VII. All these candidates have a rather narrow width of about 100 MeV in accordance with our prediction, in contrast with the $q\bar{q}$ scalar mesons, which are expected to have a very broad width of several hundred MeV in most of ordinary quark-model calculations.

It is notable that the candidates $a_0(1320)$ and $f_0(1525)$, respectively, for the a_{g0} and f_{g0}' have been observed in the respective channels $\eta\pi$ and $K\bar{K}$ with the largest branching ratios. In this connection it is interesting to check experimentally the existence of the $f_{g0}(1240)$, being observed in the $K\bar{K}$ channel with the second largest branching ratio, in the largest branching $\pi\pi$ channel.

2^{++} *nonet.* There exists only a candidate, the $f_2(1640)$ for the member f_{g2}, which has properties shown in Table VII. It has been observed in the $\omega\omega$ channel with the second largest branching ratio, but has a smaller width than our prediction.

C. Candidates for the excited hybrid mesons

Recently, in the $\pi^- p$ charge-exchange reactions, a new isoscalar $\eta\eta'$ resonance $X(1920)$ with a mass of 1911 ± 10 MeV, a width of 90 ± 35 MeV, and possible $J^{PC} = 0^{++}$, 1^{-+}, or 2^{++} has been found [35]. This meson has the unusual properties that its decays into $\eta\eta$, $\pi\pi$, and $K\bar{K}$ are strongly suppressed in comparison with its decay into $\eta\eta'$ and that it seems to be produced by a quite different mechanism from one-pion exchange. It has been pointed out [35] that these peculiarities of the $X(1920)$ would find a natural explanation if this meson had the non-$q\bar{q}$ exotic quantum numbers $J^{PC} = 1^{-+}$.

In our scheme for hybrid mesons, there exist four isoscalar 1^{-+} states in the first excited level as shown in Table III. One is a state with the $q\bar{q}$ pair being in a spin-singlet P-wave state, and the other three are states with the gluons being in P-wave states with respect to the $q\bar{q}$ pairs, which are in spin-triplet S-wave states. In our model the former, to which $X(1920)$ may be plausibly assigned, is expected to lie around a mass of about 1.8–2.2 GeV and the latter around about 2.0–2.4 GeV, according to the reasoning given in Sec. II B.

D. Further search for hybrid mesons

We now have 8 experimental candidates for the ground-state hybrid meson nonets, having 16 members in total, although further confirmation is necessary, as shown in Table VII. Here we give some comments on searching further for the missing members of their nonets by recourse to their predicted decay properties given in Table VI. First, we shall refer to the tensor nonet.

$a_{g2}(1400$–$1600)$. This state is predicted to have a prominent decay mode to $\rho\pi$ with a width of about 100–300 MeV dependent upon its mass value and so may be seen in an experiment with gluon-rich processes being sensitive to this channel. The interference effects between the a_{g2} and $^3P_2$ $q\bar{q}$ state $a_2(1320)$, mainly decaying into $\rho\pi$, could be important if the a_{g2} has a low mass value close to the $a_2(1320)$. There is also another effective decay mode of $\omega\rho$ [or $\omega(\pi\pi)_\rho$] (with a width of about 50 MeV for its mass of about 1600 MeV), if the mass of the a_{g2} is large enough to decay into this channel. In such a high-mass case, the interference effect will not be important. It may be worth noting in the opposite case of the low mass value that the existence of the a_{g2} has no effect on the observation of the $a_2(1320)$ in the $\eta\pi$ channel, because the tensor hybrid states almost decouple with the PP channel, as mentioned in Sec. III C.

$K_{g2}^*(1500$–$1700)$. Its main decay mode is predicted to

be $K^*\pi$ with a width of about 30–120 MeV, and in this channel there could be an interference effect with the $^3P_2$ $q\bar{q}$ state $K_2^*(1430)$. There are also other effective channels of $K\rho$, $K\omega$, $K^*\rho$ [or $K^*(\pi\pi)_\rho$], and $K^*\omega$, where the interference effects may be small or negligible similarly as in the case of the a_{g2}. Accordingly, the observation of the $K_2^*(1430)$ in the $K\pi$ channel will not be affected by the K_{g2}^*.

$f'_{g2}(1650–1850)$. This state is predicted to have a prominent decay mode to $K^*\bar{K}$ with a width of about 30–130 MeV and also to decay into $K^*\bar{K}^*$ if its mass is large enough. The interference between the f'_{g2} and $^3P_2$ $q\bar{q}$ state $f'_2(1525)$ will be negligible because the latter couples only with the $K\bar{K}$ and $\eta\eta$ channels, while the former almost decouples with them.

As for the axial-vector 1^{++} and 1^{+-} nonets, we have the two missing members for each nonet and have already given a comment on one of them, the $h_{g1}(1300–1500)$ in Sec. IV B.

$K_{g1}^{(A)}(1400–1600)$. Since the total width of this state is predicted to be much above 400 MeV, it will be observed only as a background effect. It is, however, noted that the candidate $K_1(1650)$ for the 1^{+-} nonet member $K_{g1}^{(B)}$ could be a mixture of the $K_{g1}^{(A)}$ and $K_{g1}^{(B)}$.

$f'_{g1}(1550–1750)$. This state is the isoscalar partner (with mainly $s\bar{s}g$ content) of our first hybrid meson $f_{g1}(1420)$, and its only simple decay channel $K^*\bar{K}$ has a broad width of about 300–400 MeV. It is possible that this state will be found by a high statistics isobar-type analysis through the interference with the $^3P_1$ $q\bar{q}$ state $f_1(1510)$.

$h'_{g1}(1550–1750)$. Since this state has also a prominent decay mode to $K^*\bar{K}$ with a width of about 50–70 MeV, it will be found together with the f'_{g1}. If its mass is large enough to decay into $\phi\eta$, this channel (with a width of about 20 MeV for its mass of about 1750 MeV) may be available.

As for the scalar 0^{++} nonet, we have the only one missing member.

$K_{g0}^*(1300–1500)$. This state is predicted to have a very narrow total width of about 50 MeV in contrast with the corresponding $^3P_0$ $q\bar{q}$ state and to couple mainly with $K\pi$. If such a narrow scalar resonance in the $K\pi$ channel is found, it will probably be the K_{g0}^*.

V. CONCLUDING REMARKS

Following the argument given in our previous work, in this paper we have supposed the $f_1(1420)$ to be one of the ground-state hybrid mesons and investigated generally the properties of the hybrid-meson system in the framework of the extended COQM. First, we have pointed out that there may occur generally an interesting fact of the doubling of the four flavor nonets with $J^{PC}=(0,1,2)^{++}$ and 1^{+-} between the ground-state hybrid mesons and the ordinary P-wave $q\bar{q}$ mesons, since the massive S-wave gluon inside the hybrid mesons plays the role of a P-wave quantum in the $q\bar{q}$ mesons, and the mass of the ground-state hybrid mesons is expected to be almost equal to that of the P-wave $q\bar{q}$ mesons. Second, based upon their predicted decay properties [which are obtained by using the width of the $f_1(1420)$ as an input], we have tried to find experimental candidates for the hybrid mesons out of unclassified observed meson resonances. The result is summarized in Table VIII. From this table we see that there may have been already observed nearly half of the members of our predicted four nonets.

Here it is to be noted that our argument vitally depends upon the supposition that the gluon inside hadrons has a nonzero effective mass. Accordingly, the ground states of our hybrid mesons have positive parity and this makes it possible to assign the $f_1(1420)$ (with positive parity) to one of their ground states. This is in strong contrast with the case of the bag model (see the discussion in Sec. II B). Here it is also to be noted that our supposition of a massive gluon makes a vital change in the decay properties of the ground-state hybrid mesons, compared to the ordinary "massless" gluon models [36]. The main decay mode of our ground-state hybrid mesons was the two ground-state $q\bar{q}$ mesons. On the one hand, in the ordinary approach based upon the bag model picture, the ground-state hybrid mesons in the TE mode cannot decay into two S-wave $q\bar{q}$ mesons, although the second lowest hybrid mesons in the TM mode (which have the same quantum numbers as our ground-state hybrid mesons) can decay into them. On the other hand, in the flux-tube model, the low-lying hybrid mesons generally have no couplings with two S-wave mesons. A physical origin for this rule seems to come from the fact that the flux-tube

TABLE VIII. Present status of our assignments for the ground-state hybrid-meson nonets.

		$I=1$	$I=\frac{1}{2}$	$I=0$	
$^{2S+1,2\Sigma+1}L_J$	J^{PC}	$n\bar{n}g$	$n\bar{s}g, s\bar{n}g$	$n\bar{n}g$	$s\bar{s}g$
$^{13}S_1$	1^{+-}	$b_{g1}(1300)$	$K_{g1}(1650)$		
$^{31}S_0$	0^{++}	$a_{g0}(1320)$		$f'_{g0}(1240)$	$f'_{g0}(1525)$
$^{33}S_1$	1^{++}	$a_{g1}(1400)$	(*)[a]	$f_{g1}(1420)$	(**)[b]
$^{35}S_2$	2^{++}			$f_{g2}(1640)$	

[a]This state is expected to be seen only as a background effect because of its very broad width.

[b]This state may be observed only through interference effects between doubling partners because of its broad width. See the text.

breaking mechanism in the model necessitates the $0^{++}(^3P_0)$ production of a new $q\bar{q}$ pair. In contrast, in the static limit of our case, a $1^{--}(^3S_1)$ $q\bar{q}$ pair is produced through the S-wave massive gluon in the initial ground-state hybrid meson. It may be worthwhile to add the following remarks: There are other plausible arguments in the level of hadron interactions, where the $f_1(1420)$ is regarded as simply a something like a meson-meson molecule [37]. However, here we should note that the two interpretations from the quark-gluon and hadron levels are not necessarily mutually exclusive: Remember the history of hadron physics and especially the fact that the Δ particle now to be regarded as a three-quark bound state had been interpreted as a resonance in the pion-nucleon system from the Chew-Low theory for a long time, the interpretation of which is still correct.

Next, we give some remarks concerning other kinds of hybrid states. Theoretically, we may expect equally the existence of various hybrid states, if our present hybrid mesons prove to truly exist. One of the most interesting ones may be hybrid mesons with heavy quarks, where we can expect equally the doubling of states. In the case of the ground-state hybrid $c\bar{c}g$ mesons, their mass is expected to be around $m_{J/\psi}+m_g \approx 3.8$ GeV (or a little lower, considering an effect of running gluon mass), while their doubling partners χ_c and h_c mesons (which are P-wave $c\bar{c}$ states) have a mass of 3.4–3.5 GeV. Thus, in this case, since the mass values of doubling states are largely separated from each other compared to their characteristic decay width of about 10 MeV or less, there may be no chance of interference between the doubling states.

In the case of baryons, the ordinary P-wave qqq states, which belong to the $(70,1^-)$ multiplet of $SU(6)\otimes O(3)_L$, have rather too complicated level structures, as a result of the freedom of two relative coordinates and the quark flavor-spin symmetry, to be simply compared to those of the ground-state hybrid $qqqg$ baryons.

ACKNOWLEDGMENTS

We would like to thank Professor K. Takamatsu, Professor T. Tsuru, I. Yamauchi, and their collaborators at KEK for useful communication and discussions. We are also grateful to N. Honzawa and M. Sekiguchi for their support. We thank Professor O. Hara and the other members of the particle physics group of Atomic Energy Research Institute for encouragement.

APPENDIX A: SPACE-TIME OVERLAP INTEGRAL

The coupling constants in the effective decay Hamiltonians shown in Table IV are obtained through the overlap integral in Eq. (3.1). Here we give the results of the space-time integral. It involves the integrals

$$J_\mu^E(J_\nu^M)=\int d^4x_1 d^4x_2 d^4x_3[\Phi_C^*(x_3,x_2)O_\mu^E(O_\nu^M)\Phi_B^*(x_1,x_3)]H(x_1,x_2,x_3)\ , \tag{A1}$$

with

$$O_\mu^E=-ig\frac{1}{2m_p}\left[\frac{\vec{\partial}}{\partial x_{3\mu}}-\frac{\overleftarrow{\partial}}{\partial x_{3\mu}}\right], \tag{A2}$$

$$O_\nu^M=-ig\frac{h_M}{2m_p}\left[\frac{\vec{\partial}}{\partial x_{3\mu}}+\frac{\overleftarrow{\partial}}{\partial x_{3\mu}}\right], \tag{A3}$$

where O_μ^E [O_ν^M] is the space-time factor of the operator Γ^E [Γ^M] given in Eq. (3.3a) [(3.3b)] and H [Φ_B and Φ_C] means the space-time part of the wave function for initial hybrid [final $q\bar{q}$] mesons given in Eq. (3.4a) [(3.4b)]. Defining

$$J_\mu^B=\int d^4x_1 d^4x_2 d^4x_3\Phi_C^*(x_3,x_2)\left[\frac{\partial}{\partial x_{3\mu}}\Phi_B^*(x_1,x_3)\right]H(x_1,x_2,x_3) \tag{A4}$$

and

$$J_\mu^C=\int d^4x_1 d^4x_2 d^4x_3\left[\frac{\partial}{\partial x_{3\mu}}\Phi_C^*(x_3,x_2)\right]\Phi_B^*(x_1,x_3)H(x_1,x_2,x_3)\ , \tag{A5}$$

the relevant integrals in Eq. (A1) are given as

$$J_\mu^E=-ig\frac{1}{2m_p}(J_\mu^B-J_\mu^C)\ , \tag{A6}$$

$$J_\nu^M=-ig\frac{h_M}{2m_p}(J_\nu^B+J_\nu^C)\ . \tag{A7}$$

For the evaluation of the integrals in Eqs. (A4) and (A5), we choose X_H, x_B ($=x_1-x_3$), and x_C ($=x_3-x_2$) as the variables of integration. Then, performing the integration with respect to X_H, we obtain

$$J_\mu^B=N(2\pi)^4\delta^4(P_H-P_B-P_C)(-i)\left[\left[\frac{m_p}{m+m_p}F+2\frac{\beta_B}{M_B^2}P_B\cdot G^B\right]P_{B\mu}+\beta_B G_\mu^B\right] \tag{A8}$$

and

$$J_\mu^C = N(2\pi)^4\delta^4(P_H - P_B - P_C)(-i)\left[\left[\frac{m_p}{m+m_p}F - 2\frac{\beta_C}{M_C^2}P_C\cdot G^C\right]P_{C\mu} - \beta_C G_\mu^C\right], \tag{A9}$$

where

$$F(P_H,P_B,P_C) \equiv \int d^4x_B d^4x_C e^{i(Q_B\cdot x_B + Q_C\cdot x_C)}\Psi_C^*(x_C;P_C)\Psi_B^*(x_B;P_B)\Psi_H(x_B,x_C;P_H)\,, \tag{A10}$$

$$G_\mu^B(P_H,P_B,P_C) \equiv \int d^4x_B d^4x_C (ix_{B\mu}) e^{i(Q_B\cdot x_B + Q_C\cdot x_C)}\Psi_C^*(x_C;P_C)\Psi_B^*(x_B;P_B)\Psi_H(x_B,x_C;P_H)\,, \tag{A11}$$

$$G_\mu^C(P_H,P_B,P_C) \equiv \int d^4x_B d^4x_C (ix_{C\mu}) e^{i(Q_B\cdot x_B + Q_C\cdot x_C)}\Psi_C^*(x_C;P_C)\Psi_B^*(x_B;P_B)\Psi_H(x_B,x_C;P_H)\,, \tag{A12}$$

with

$$Q_B = -\frac{m}{2m+m_g}\left[\frac{m-m_p+m_g}{m+m_p}P_B - P_C\right], \tag{A13}$$

$$Q_C = -\frac{m}{2m+m_g}\left[P_B - \frac{m-m_p+m_g}{m+m_p}P_C\right] \tag{A14}$$

and

$$N = [(2\pi)^3 2E_H (2\pi)^3 2E_B (2\pi)^3 2E_C]^{-1/2}\,. \tag{A15}$$

The Lorentz-invariant integral F in Eq. (A10) is given, in the special case of $M_B = M_C$, as

$$F = \frac{32\alpha_\rho\alpha_\lambda\beta^2}{(\alpha_\rho+\beta)(\alpha_\lambda/3+\beta)[2(\alpha_\rho-\beta)(\alpha_\lambda/3-\beta)+\beta(\alpha_\rho+\alpha_\lambda/3)M_H^2/M_B^2]}$$
$$\times\exp\left[-\frac{[m/(m+m_p)]^2 M_B^2}{4(\alpha_\rho-\beta)(\alpha_\lambda/3-\beta)+2\beta(\alpha_\rho+\alpha_\lambda/3)M_H^2/M_B^2}\right.$$
$$\left.\times\left\{\left[\frac{\alpha_\lambda}{3}-\beta+2\beta\left[\frac{m+m_p}{2m+m_g}\right]^2\frac{M_H^2}{M_B^2}\right]\left[\frac{M_H^2}{M_B^2}-4\right]+(\alpha_\rho+\beta)\left[\frac{2m_p-m_g}{2m+m_g}\right]^2\frac{M_H^2}{M_B^2}\right\}\right], \tag{A16}$$

where $\beta \equiv \beta_B = \beta_C$ and we have used energy-momentum conservation and the relations $P_{i\mu}^2 = -M_i^2$ $(i = H,B,C)$. We also find for the integrals G_μ^B and G_μ^C that

$$G_\mu^B = G_-(P_{B\mu} - P_{C\mu}) + G_+(P_{B\mu} + P_{C\mu})\,, \tag{A17}$$

$$G_\mu^C = G_-(P_{B\mu} - P_{C\mu}) - G_+(P_{B\mu} + P_{C\mu})\,, \tag{A18}$$

where G_- and G_+, being Lorentz-invariant quantities, are

$$G_- = \frac{1}{2(\alpha_\rho-\beta)(\alpha_\lambda/3-\beta)+\beta(\alpha_\rho+\alpha_\lambda/3)M_H^2/M_B^2}\left[\frac{m}{m+m_p}\right]\left[\frac{\alpha_\lambda}{3}-\beta+\beta\left[\frac{m+m_p}{2m+m_g}\right]\frac{M_H^2}{M_B^2}\right]F \tag{A19}$$

and

$$G_+ = \frac{1}{2(\alpha_\rho-\beta)(\alpha_\lambda/3-\beta)+\beta(\alpha_\rho+\alpha_\lambda/3)M_H^2/M_B^2}\left[\frac{m}{m+m_p}\right]\left[\frac{2m_p-m_g}{2m+m_g}(\alpha_\rho+\beta)+\beta\left[\frac{m+m_p}{2m+m_g}\right]\left[\frac{M_H^2}{M_B^2}-4\right]\right]F\,, \tag{A20}$$

with F given in Eq. (A16).

Here, for the sake of calculational convenience, we write J_μ^E and J_ν^M as

$$J_\mu^E = A_0(-iP_{B\mu}) + A_1(-iP_{H\mu})\,, \tag{A21}$$

$$J_\nu^M = B_0(-iP_{B\nu}) + B_1(-iP_{H\nu})\,, \tag{A22}$$

where, in the special case of $M_B = M_C$,

$$A_0=\frac{g}{m_p}\left[\frac{m_p}{m+m_p}F+\beta\left\{\left[\frac{M_H^2}{M_B^2}-2\right]G_-+\frac{M_H^2}{M_B^2}G_+\right\}\right], \tag{A23}$$

$$A_1=-\tfrac{1}{2}A_0\ , \tag{A24}$$

$$B_0=0\ , \tag{A25}$$

$$B_1=\frac{gh_M}{2m_p}\left[\frac{m_p}{m+m_p}F+\beta\left\{\left[\frac{M_H^2}{M_B^2}+2\right]G_-+\frac{1}{2}\left[\frac{M_H^2}{M_B^2}-4\right]G_+\right\}\right]. \tag{A26}$$

Thus far, we have concerned ourselves with the first term of the overlap integral in Eq. (3.1). The space-time integral parts $\overline{J_\mu^E}$ and $\overline{J_\nu^M}$ of the second term, being the Hermitian conjugate of the first term, are related to J_μ^E and J_ν^M as

$$\overline{J_\mu^E}=-J_\mu^E\ ,\quad \overline{J_\nu^M}=J_\nu^M\ . \tag{A27}$$

APPENDIX B: COUPLING CONSTANTS IN THE EFFECTIVE DECAY HAMILTONIANS

We can express coupling constants appearing in the effective decay Hamiltonians in terms of M_H, M_B, and M_C (symmetric masses of hybrid and ordinary mesons) and A_0, A_1, B_0, and B_1 defined in Eqs. (A23)–(A26). Their expressions for each decay process are as follows.

$B\to V+P$ process:

$$g_{BVP}^{(1)}=\frac{1}{4\sqrt{2}}\left[\frac{(M_H+M_B+M_C)[M_B(P_BP_C)-M_B^2M_C]}{M_BM_CM_H}B_0+\frac{(M_BM_H+M_CM_H+M_B^2+M_C^2)(P_BP_C)}{M_BM_CM_H}B_1\right.$$
$$\left.-\frac{M_BM_C(M_H^2+M_BM_H+M_CM_H+2M_BM_C)}{M_BM_CM_H}B_1\right], \tag{B1}$$

$$g_{BVP}^{(2)}=\frac{1}{4\sqrt{2}}\left[-\frac{M_H+M_B+M_C}{M_CM_H}A_0-\frac{(M_B-M_C)(M_B+M_C+M_H)}{M_BM_CM_H}B_1\right]. \tag{B2}$$

$B\to V+V$ process:

$$g_{BVV}^{(1)}=\frac{1}{4\sqrt{2}}\left[G_0\left[1-\frac{(P_CP_H)}{M_CM_H}\right]+\frac{G_0M_B^2-(2G_0+G_1)(P_BP_C)+2G_1M_C^2}{2M_BM_C}-\frac{G_0M_B^2-G_1(P_BP_C)}{2M_BM_H}\right], \tag{B3}$$

$$g_{BVV}^{(2)}=\frac{1}{4\sqrt{2}}\left[G_1\left[1-\frac{(P_CP_H)}{M_CM_H}\right]-\frac{(M_H+M_C)[G_0M_B^2-G_1(P_BP_c)]}{2M_BM_CM_H}\right], \tag{B4}$$

$$g_{BVV}^{(3)}=\frac{1}{4\sqrt{2}}\left[G_0\frac{2M_B+M_C+M_H}{2M_BM_CM_H}+\frac{G_1}{M_BM_C}\right], \tag{B5}$$

$$g_{BVV}^{(4)}=\frac{1}{4\sqrt{2}}\left[\frac{M_B+M_C-M_H}{M_BM_CM_H}A_0+G_0\frac{M_H+M_C}{2M_BM_CM_H}\right], \tag{B6}$$

$$g_{BVV}^{(5)}=\frac{1}{4\sqrt{2}}\frac{M_H+2M_B-M_C}{2M_BM_CM_H}G_1\ , \tag{B7}$$

where $G_0=A_0+A_1$ and $G_1=A_1$.

$S\to P+P$ process:

$$g_{SPP}^{(1)}=\frac{1}{8\sqrt{2}}\frac{M_H+M_B+M_C}{M_BM_CM_H}\{M_B[M_H^2-(M_B+M_C)^2]B_0+(M_B+M_C)M_H^2-(M_B^2-M_C^2)B_1\}\ , \tag{B8}$$

$$g_{SPP}^{(2)}=\frac{1}{4\sqrt{2}}\left[\frac{M_B+M_C-M_H}{M_BM_C}A_0-\frac{(M_B-M_C)(M_B+M_C+M_H)}{M_BM_CM_H}B_0\right]. \tag{B9}$$

$S \to V + V$ process:

$$g^{(1)}_{SVV} = \frac{1}{4\sqrt{2}} \left[\frac{M_B + M_C + M_H}{M_B M_C} A_0 + 3 \frac{G_0(P_B P_H) + G_1(P_C P_H)}{M_H M_B^2} + \left[1 - \frac{(P_B P_H)}{M_B M_H} \right] \frac{(G_0 - G_1)(P_B P_C) - 3[G_0(P_B P_C) - G_1 M_C^2]}{M_B^2 M_C} - \left[1 - \frac{(P_C P_H)}{M_C M_H} \right] \frac{(G_0 - G_1)(P_B P_C) + 3[G_0 M_B^2 - G_1(P_B P_C)]}{M_B M_C^2} + \frac{G_0(P_B P_H) + G_1(P_C P_H)}{M_B^2 M_C^2 M_H} \left[M_B^2 + \frac{1}{3}(P_B P_C) \right] \right], \tag{B10}$$

$$g^{(2)}_{SVV} = \frac{1}{4\sqrt{2}} \left[\frac{2}{M_B M_C M_H} A_0(P_B P_C) + 3 \left[1 - \frac{(P_B P_H)}{M_B M_H} \right] \frac{G_0}{M_C} + 3 \left[1 - \frac{(P_C P_H)}{M_C M_H} \right] \frac{G_1}{M_B} + \frac{(G_0 + G_1)(P_B P_C) - 3[G_0 M_B^2 - 2G_1(P_B P_C)]}{M_B M_C M_H} + \frac{3}{2} \frac{G_0(P_B P_H) + G_1(P_C P_H)}{M_B M_C M_H} + \frac{(G_0 - 2G_1)(P_B P_C)}{M_B M_C M_H} \right], \tag{B11}$$

$$g^{(3)}_{SVV} = \frac{1}{4\sqrt{2}} \left[\frac{2}{M_B M_C M_H} [G_0(P_B P_H) + G_1(P_C P_H)] + \left[1 - \frac{(P_B P_H)}{M_B M_H} \right] \frac{2}{M_C} [G_0(P_B P_C) - G_1 M_C^2] - 2 \left[1 - \frac{(P_C P_H)}{M_C M_H} \right] \frac{G_0 M_B^2 - G_1(P_B P_C)}{M_B} + \frac{G_0(P_B P_H) + G_1(P_C P_H)}{M_B M_C M_H} (P_B P_C) \right], \tag{B12}$$

$$g^{(4)}_{SVV} = \frac{1}{4\sqrt{2}} \left[- \frac{M_B + M_C + M_H}{M_B M_H} A_0 + \frac{G_0(P_B P_H) + G_1(P_C P_H)}{M_H M_B M_C} + 2 \left[1 - \frac{(P_B P_H)}{M_B M_H} \right] \frac{G_0}{M_C} - \left[1 - \frac{(P_C P_H)}{M_C M_H} \right] \frac{G_0 - G_1}{M_B} + \frac{G_0[2M_B^2 - (P_B P_C)] - G_1(P_B P_C)}{M_B M_C M_H} \right], \tag{B13}$$

$$g^{(5)}_{SVV} = \frac{1}{4\sqrt{2}} \left[- \frac{M_B + M_C + M_H}{M_C M_H} A_0 + \left[1 - \frac{(P_B P_H)}{M_B M_H} \right] \frac{G_0 - G_1}{M_C} - 2 \left[1 - \frac{(P_C P_H)}{M_C M_H} \right] \frac{G_1}{M_B} - \frac{G_0(P_B P_H) + G_1(P_C P_H) - (G_0 + G_1)(P_B P_C) + 2G_1 M_C^2}{M_B M_C M_H} \right]. \tag{B14}$$

$A \to V + P$ process:

$$g^{(1)}_{AVP} = \frac{1}{4\sqrt{2}} \left[\frac{M_H B_1 - 3M_B B_0}{2M_H M_B M_C} - \frac{M_H + M_B + M_C}{M_B M_C M_H} A_0 \right], \tag{B15}$$

$$g^{(2)}_{AVP} = \frac{1}{4\sqrt{2}} \frac{M_H + 2M_B - M_C}{2M_H M_B M_C} B_1, \tag{B16}$$

$$g^{(3)}_{AVP} = \frac{1}{4\sqrt{2}} \left[\left[1 + \frac{(P_C P_H)}{M_C M_H} B_0 \right] - \frac{(M_C - M_H)[B_0(P_B P_H) - B_1 M_H^2]}{2M_H M_B M_C} + \frac{M_H[B_0 M_B^2 - B_1(P_B P_H)]}{2M_H M_B M_C} \right], \tag{B17}$$

$$g^{(4)}_{AVP} = \frac{1}{4\sqrt{2}} \left[\left[1 + \frac{(P_C P_H)}{M_C M_H} B_1 \right] - \frac{B_0 M_B^2 - B_1 P_B P_H}{2M_H M_B} \right]. \tag{B18}$$

$A \to V + V$ process:

$$g^{(1)}_{AVV} = \frac{1}{4\sqrt{2}} \left[- \frac{M_B + M_C + M_H}{M_B M_H} A_0 - \left[1 - \frac{(P_C P_H)}{M_C M_H} \right] \frac{B_0}{M_B} - \left\{ \frac{B_0}{M_H} + 2 \left[1 - \frac{(P_C P_H)}{M_C M_H} \right] \frac{B_1}{M_B} + 2 \frac{B_0(P_B P_C) + B_1(P_C P_H)}{M_H M_B M_C} \right\} + \frac{(P_B P_C)}{M_B M_C M_H} B_0 \right], \tag{B19}$$

$$g^{(2)}_{AVV}=\frac{1}{4\sqrt{2}}\left[\frac{M_B+M_C+M_H}{M_BM_H}A_0+\left[1-\frac{(P_BP_C)}{M_BM_H}\right]\frac{B_0}{M_H}+2\left[1-\frac{(P_BP_H)}{M_BM_H}\right]\frac{B_1}{M_C}-2\frac{B_0M_B^2-B_1(P_BP_H)}{M_HM_BM_C}\right.$$
$$\left.+\left[1-\frac{(P_BP_H)}{M_BM_H}\right]\frac{B_0}{M_C}\right]. \tag{B20}$$

$T\to P+P$ process:

$$g_{TPP}=\frac{1}{4\sqrt{2}}\left[\frac{M_B+M_C-M_H}{M_BM_C}A_0+\frac{(M_C-M_B)(M_B+M_C+M_H)}{M_BM_CM_H}B_0\right]. \tag{B21}$$

$T\to V+P$ process:

$$g_{TVP}=\frac{1}{4\sqrt{2}}\left[\frac{M_H+M_B-M_C}{M_BM_CM_H}A_0+\frac{(M_B+2M_C)B_0+3M_HB_1}{2M_BM_CM_H}\right]. \tag{B22}$$

$T\to V+V$ process:

$$g^{(1)}_{TVV}=\frac{1}{4\sqrt{2}}\left[2\frac{B_0(P_BP_H)-B_1M_H^2}{M_H}+4\left[1-\frac{(P_BP_H)}{M_BM_H}\right]\frac{B_0(P_BP_C)+B_1(P_HP_C)}{M_C}\right.$$
$$\left.-4\left[1-\frac{(P_CP_H)}{M_CM_H}\right]\frac{B_0M_B^2-B_1(P_HP_B)}{M_B}+\frac{B_0(P_BP_H)-B_1M_H^2}{M_BM_CM_H}(P_BP_C)\right], \tag{B23}$$

$$g^{(2)}_{TVV}=\frac{1}{4\sqrt{2}}\left[\frac{M_B+M_C+M_H}{M_BM_C}A_0-\left[1-\frac{(P_BP_H)}{M_BM_H}\right]\frac{B_0}{M_C}+\left[1-\frac{(P_CP_H)}{M_CM_H}\right]\frac{B_0}{M_B}-\frac{B_0(P_BP_H)-B_1M_H^2}{M_BM_CM_H}\right], \tag{B24}$$

$$g^{(3)}_{TVV}=\frac{1}{4\sqrt{2}}\left[-\frac{M_B+M_C+M_H}{M_BM_C}A_0+2\left[1-\frac{(P_BP_H)}{M_BM_H}\right]\frac{B_0+B_1}{M_C}-\left[1-\frac{(P_CP_H)}{M_CM_H}\right]\frac{B_0}{M_B}\right.$$
$$\left.-\frac{B_0}{M_H}-\frac{B_0(P_BP_H)-B_1M_H^2}{M_BM_CM_H}+2\frac{B_0M_B^2-B_1(P_HP_B)}{M_BM_CM_H}-\frac{B_0(P_BP_C)}{M_BM_CM_H}\right], \tag{B25}$$

$$g^{(4)}_{TVV}=\frac{1}{4\sqrt{2}}\left[\frac{M_B+M_C+M_H}{M_BM_C}A_0-\left[1-\frac{(P_BP_H)}{M_BM_H}\right]\frac{B_0}{M_C}-\left[1-\frac{(P_CP_H)}{M_CM_H}\right]\frac{B_0}{M_B}\right.$$
$$\left.+\frac{B_0}{M_H}-\frac{B_0(P_BP_H)-B_1M_H^2}{M_BM_CM_H}+2\frac{B_0(P_BP_C)+B_1(P_HP_C)}{M_BM_CM_H}-\frac{B_0(P_BP_C)}{M_BM_CM_H}\right], \tag{B26}$$

$$g^{(5)}_{TVV}=\frac{1}{2\sqrt{2}}\frac{A_0+B_0+2B_1}{M_BM_CM_H}. \tag{B27}$$

Here the Lorentz-invariant quantities (P_BP_C), (P_HP_B), and (P_HP_C) appearing in these expressions are written as

$$(P_BP_C)=\tfrac{1}{2}(M_B^2+M_C^2-M_H^2),\quad (P_HP_B)=\tfrac{1}{2}(M_A^2-M_B^2-M_H^2),\quad (P_HP_C)=\tfrac{1}{2}(M_B^2-M_A^2-M_H^2). \tag{B28}$$

It is noted that the effective coupling constants are written in terms of our model parameters g, h_M, K, m_q, m_g, M_H, and M_i. The numerical results for respective decay widths given in Table VI are obtained by taking the following values of these parameters:

$g=6.6$ GeV , $h_M=1.69$,

for the fundamental coupling constants g and h_M,

$\Omega_{n\bar{n}}=1.15$ GeV^2 ,

for $\Omega_{n\bar{n}}=\sqrt{32m_nK}$, instead of the confining strength K,

$m_n=385$ MeV , $m_s=510$ MeV , $m_g=700$ MeV ,

for the effective quark and gluon masses,

$$M_H(n\bar{n}g)=M_H(n\bar{s}g \text{ or } s\bar{n}g)=1.90 \text{ GeV}\ ,\quad M_H(s\bar{s}g)=2.15 \text{ GeV}\ ,$$

for the symmetric masses of the ground-state hybrid mesons, and

$$M(n\bar{n})=0.77 \text{ GeV}\ ,\quad M(n\bar{s} \text{ or } s\bar{n})=0.91 \text{ GeV}\ ,\quad M(s\bar{s})=1.02 \text{ GeV}\ ,$$

for the symmetric masses of S-wave $q\bar{q}$ mesons.

[1] For recent reviews, see, for example, F. E. Close, Rep. Prog. Phys. **51**, 833 (1988); L. G. Landsberg, Usp. Fiz. Nauk **160**, 1 (1990) [Sov. Phys. Usp. **33**, 169 (1990)]; T. H. Burnett and S. R. Sharpe, Annu. Rev. Nucl. Part. Sci. **40**, 327 (1990).

[2] For recent reviews, see, for example, Landsberg [1]; Particle Data Group, J. J. Hernández *et al.*, Phys. Lett. B **239**, 1 (1990); see, in particular, the minireview on non-$q\bar{q}$ candidates, p. VII. 165.

[3] S. Ishida *et al.*, Prog. Theor. Phys. **82**, 119 (1989). See also K. Yamada *et al.*, in *Hadron '89,* Proceedings of the Third International Conference on Hadron Spectroscopy, Ajaccio, France, 1989, edited by F. Binon, J.-M. Frere, and J.-P. Peigneux (Editions Frontieres, Gif-sur-Yvette, 1989), p. 305.

[4] S. Ishida, Prog. Theor. Phys. **46**, 1570 (1971); **46**, 1905 (1971); R. P. Feynman, M. Kislinger, and F. Ravndal, Phys. Rev. D **3**, 2706 (1971). For a review, see S. Ishida, in *Hadron Spectroscopy—1985,* Proceedings of the First International Conference on Hadron Spectroscopy, University of Maryland, edited by S. Oneda, AIP Conf. Proc. No. 132 (AIP, New York, 1985), p. 277, and references therein. See also Y. S. Kim and M. E. Noz, *Theory and Applications of the Poincaré Group* (Reidel, Dordrecht, 1986).

[5] D. Horn and J. Mandula, Phys. Rev. D **17**, 898 (1978); K. F. Liu and C. W. Wong, *ibid.* **21**, 1350 (1980); T. Kitazoe *et al.*, Z. Phys. C **24**, 143 (1984). In these papers hybrid mesons containing heavy quarks only were examined. The constituent gluon was treated as a massless vector particle in the first two papers. For works on light-quark hybrid mesons, see A. S. de Castro and H. F. de Carvalho, J. Phys. G **16**, L81 (1990); S. Bhatnagar and A. N. Mitra, Nuovo Cimento A **104**, 925 (1991).

[6] As for light-quark hybrid mesons, thus far, there have been published many works from other approaches: For the bag-model approach, see T. Barnes, Nucl. Phys. **B158**, 171 (1979); F. de Viron and J. Weyers, *ibid.* **B185**, 391 (1981); T. Barnes and F. E. Close, Phys. Lett. **116B**, 365 (1982); M. Chanowitz and S. Sharpe, Nucl. Phys. **B222**, 211 (1983); T. Barnes, F. E. Close, and F. de Viron, *ibid.* **B224**, 241 (1983); M. Flensburg, C. Peterson, and L. Sköld, Z. Phys. C **22**, 293 (1984). For the flux-tube-model approach, see N. Isgur and J. Paton, Phys. Lett. **124B**, 247 (1983); Phys. Rev. D **31**, 2910 (1985); J. Merlin and J. Paton, J. Phys. G **11**, 439 (1985); Phys. Rev. D **35**, 1668 (1987). For the QCD sum-rule approach, see I. I. Balitsky, D. I. Dyakonov, and A. V. Yung, Yad. Fiz. **35**, 1300 (1982) [Sov. J. Nucl. Phys. **35**, 761 (1982)]; Phys. Lett. **112B**, 71 (1982); Z. Phys. C **33**, 265 (1986); J. Govaerts, F. de Viron, D. Gusbin, and J. Weyers, Phys. Lett. **128B**, 262 (1983); Nucl. Phys. **B248**, 1 (1984); J. I. Latorre, S. Narison, P. Pascual, and R. Tarrach, Phys. Lett. **147B**, 169 (1984); J. Govaerts, L. J. Reinders, and J. Weyers, Nucl. Phys. **B262**, 575 (1985); J. I. Latorre, P. Pascual, and S. Narison, Z. Phys. C **34**, 347 (1987); V. M. Braun and A. V. Kolesnichenko, Yad. Fiz. **44**, 756 (1986) [Sov. J. Nucl. Phys. **44**, 489 (1986)]. See also J. M. Cornwall and S. F. Tuan, Phys. Lett. **136B**, 110 (1984).

[7] J. M. Cornwall, Nucl. Phys. **B157**, 392 (1979); Phys. Rev. D **26**, 1453 (1982). For further study, see F. R. Graziani, Z. Phys. C **33**, 397 (1987); V. P. Spiridonov and K. G. Chetyrkin, Yad. Fiz. **47**, 818 (1988) [Sov. J. Nucl. Phys. **47**, 522 (1988)]; M. Lavelle, Phys. Rev. D **44**, R26 (1991).

[8] J. E. Mandula and M. Ogilvie, Phys. Lett. B **185**, 127 (1987); R. Gupta *et al.*, Phys. Rev. D **36**, 2813 (1987). For another definition of the effective gluon mass, see C. Bernard, Phys. Lett. **108B**, 431 (1982); Nucl. Phys. **B219**, 341 (1983).

[9] G. Parisi and R. Petronzio, Phys. Lett. **94B**, 51 (1980); J. F. Donoghue, Phys. Rev. D **29**, 2559 (1984).

[10] A. Salam, R. Delbourgo, and J. Strathdee, Proc. R. Soc. London **A284**, 146 (1965); B. Sakita and K. C. Wali, Phys. Rev. **139**, B1355 (1965).

[11] S. Ishida and T. Sonoda, Prog. Theor. Phys. **70**, 1323 (1983).

[12] T. Takabayasi, Nuovo Cimento **33**, 668 (1964); S. Ishida and J. Otokozawa, Prog. Theor. Phys. **47**, 2117 (1972); Y. S. Kim and M. E. Noz, Phys. Rev. D **8**, 3521 (1973).

[13] K. Fujimura, T. Kobayashi, and M. Namiki, Prog. Theor. Phys. **43**, 73 (1970); S. Ishida *et al.*, Phys. Rev. D **20**, 2906 (1979).

[14] de Viron and Weyers [6]; Barnes and Close [6]; Chanowitz and Sharpe [6]; Barnes, Close, and de Viron [6]; Flensburg, Peterson, and Sköld [6].

[15] M. S. Chanowitz, Phys. Lett. B **187**, 409 (1987).

[16] Horn and Mandula [5]; M. Tanimoto, Phys. Lett. **116B**, 198 (1982); Phys. Rev. D **27**, 2648 (1983); Barnes, Close, and de Viron [6]; A. Le Yaouanc *et al.*, Z. Phys. C **28**, 309 (1985).

[17] S. Ishida and K. Yamada, Phys. Rev. D **35**, 265 (1987).

[18] F. E. Low, Phys. Rev. D **12**, 163 (1975); S. Nussinov, Phys. Rev. Lett. **34**, 1286 (1975); Phys. Rev. D **14**, 246 (1976).

[19] S. D. Drell and K. Hiida, Phys. Rev. Lett. **7**, 199 (1961); R. T. Deck, *ibid.* **13**, 169 (1964).

[20] H. Aihara *et al.*, Phys. Rev. Lett. **57**, 2500 (1986); Phys. Rev. D **38**, 1 (1988); G. Gidal *et al.*, Phys. Rev. Lett. **59**, 2016 (1987); H.-J. Behrend *et al.*, Z. Phys. C **42**, 367 (1989); P. Hill *et al.*, *ibid.* **42**, 355 (1989).

[21] J. J. Becker *et al.*, Phys. Rev. Lett. **59**, 186 (1987); Z. Bai *et al.*, *ibid.* **65**, 2507 (1990).

[22] H. Primakoff, Phys. Rev. **81**, 899 (1951).

[23] M. Oda, S. Ishida, and K. Yamada, in *Hadron '89* [3], p. 397; T. Ferbel, in *ibid.*, p. 157; M. Zielinski *et al.*, Z. Phys.

C **31**, 545 (1986); M. Zielinski, *ibid.* **34**, 255 (1987).
[24] S. Ishida *et al.*, Prog. Theor. Phys. **88**, 89 (1992). Preliminary results of this work have been presented by one of us (H.S.) in *Hadron '91,* Proceedings of the Fourth International Conference on Hadron Spectroscopy, College Park, Maryland, 1991, edited by S. Oneda and D. C. Peaslee (World Scientific, Singapore, 1992), p. 477.
[25] S. Fukui *et al.*, Phys. Lett. B **257**, 241 (1991).
[26] S. Fukui *et al.*, KEK Report No. 90-191, 1991 (unpublished).
[27] S. Fukui *et al.*, Phys. Lett. B **267**, 293 (1991).
[28] Particle Data Group [2].
[29] M. Atkinson *et al.*, Nucl. Phys. **B242**, 269 (1984).
[30] A. Ando *et al.*, Phys. Lett. B **291**, 496 (1992).
[31] C. Daum *et al.*, Nucl. Phys. **B182**, 269 (1981).
[32] T. A. Armstrong *et al.*, Z. Phys. C **48**, 213 (1990).
[33] W. Ruckstuhl *et al.*, Phys. Rev. Lett. **56**, 2132 (1986); W. B. Schmidke *et al.*, *ibid.* **57**, 527 (1986); H. Albrecht *et al.*, Z. Phys. C **33**, 7 (1986); H. R. Band *et al.*, Phys. Lett. B **198**, 297 (1987).
[34] The possible solutions (from other viewpoints than ours) were discussed in the following papers: M. G. Bowler, Phys. Lett. B **182**, 400 (1986); **184**, 419(E) (1987); **209**, 99 (1988); N. A. Törnqvist, Z. Phys. C **36**, 695 (1987); **40**, 632(E) (1988); N. Isgur, C. Morningstar, and C. Reader, Phys. Rev. D **39**, 1357 (1989); J. Iizuka, H. Koibuchi, and F. Masuda, *ibid.* **39**, 3357 (1989); Yu. P. Ivanov, A. A. Osipov, and M. K. Volkov, Z. Phys. C **49**, 563 (1991).
[35] D. Alde *et al.*, Phys. Lett. B **216**, 447 (1989); Yu. D. Prokoshkin, in *Hadron '89* [3], p. 27.
[36] Le Yaouanc *et al.* [16]; N. Isgur, R. Kokoski, and J. Paton, Phys. Rev. Lett. **54**, 869 (1985).
[37] R. S. Longacre, Phys. Rev. D **42**, 874 (1990); N. A. Törnqvist, Phys. Rev. Lett. **67**, 556 (1991).